

This is an Open Access document downloaded from ORCA, Cardiff University's institutional repository: <https://orca.cardiff.ac.uk/id/eprint/99016/>

This is the author's version of a work that was submitted to / accepted for publication.

Citation for final published version:

Marinelli, Davide, Fasano, Francesco, Najjari, Btissam, Demitri, Nicola and Bonifazi, Davide 2017. Borazino-doped polyphenylenes. *Journal of the American Chemical Society* 139 (15) , pp. 5503-5519. 10.1021/jacs.7b01477

Publishers page: <http://dx.doi.org/10.1021/jacs.7b01477>

Please note:

Changes made as a result of publishing processes such as copy-editing, formatting and page numbers may not be reflected in this version. For the definitive version of this publication, please refer to the published source. You are advised to consult the publisher's version if you wish to cite this paper.

This version is being made available in accordance with publisher policies. See <http://orca.cf.ac.uk/policies.html> for usage policies. Copyright and moral rights for publications made available in ORCA are retained by the copyright holders.



Borazino-doped polyphenylenes

Davide Marinelli,^{†,‡} Francesco Fasano,^{†,‡} Btissam Najjari,[§] Nicola Demitri,[#] and Davide Bonifazi^{†,§,*}

[*] [†] D. Marinelli, F. Fasano, Prof. Dr. D. Bonifazi

School of Chemistry, Cardiff University, Park Place Main Building, Cardiff, CF10 3AT, United Kingdom.

E-mail: bonifazid@cardiff.ac.uk.

Dr. B. Najjari, Prof. Dr. D. Bonifazi

Department of Chemistry, University of Namur (UNamur), Rue de Bruxelles 61, Namur 5000, Belgium.

Dr. N. Demitri

Elettra – Sincrotrone Trieste, S.S. 14 Km 163,5 in Area Science Park, 34149 Basovizza, Trieste, Italy

KEYWORDS: borazines, polyphenylenes, cycloadditions, BN, heteroatom doping, boron and nitrogen, emission.

ABSTRACT: The divergent synthesis of two series of borazino-doped polyphenylenes, in which one or more aryl units are replaced by borazine rings, is reported for the first time taking advantage of the decarbonylative [4+2] Diels-Alder cycloaddition reaction between ethynyl and tetraphenylcyclopentadienone derivatives. Owing to the possibility of functionalizing the borazine core with different groups on the aryl substituents at the *N* and *B* atoms of the borazino core, we have prepared borazino-doped polyphenylenes featuring different doping dosages and orientations. To achieve it, two molecular modules were prepared: a core and a branching unit. Depending on the chemical nature of the central aromatic module and of the reactive group, each covalent combination of the modules yields one exclusive doping pattern. Indulging this approach, three- and hexa-branched hybrid polyphenylenes featuring controlled orientation and dosages of the doping B₃N₃-rings have been prepared. Detailed photophysical investigations showed that upon increasing the doping dosage, the strong luminescent signal is progressively reduced. This suggests that the presence of the B₃N₃-rings engages additional deactivation pathways possibly involving excited states with an increasing charge separate character that are restricted in the full-carbon analogues. Notably, a strong effect of the orientational doping on the fluorescence quantum yields was observed for those hybrid polyphenylene structures featuring low doping dosages. At last, we showed that Cu-catalyzed 1,3-dipolar cycloaddition is also chemically compatible with the BN core, further endorsing the inorganic benzene as a versatile aromatic scaffold to engineering molecular materials with tailored and exploitable optoelectronic properties.

Introduction

Replacing carbon by isostructural atoms is developing as a versatile functionalization strategy to tailor the optoelectronic properties of polycyclic aromatic hydrocarbons without significant structural perturbation of the nanostructure.^{1,2} Among the different dopants,¹⁻⁴ the substitution of C=C bonds by isoelectronic BN covalent couples⁵⁻¹² leads to isostructural molecular¹³⁻²⁵ and polymeric mimics²⁶⁻³³ bearing strong local dipole moments.³⁴ This imparts a series of physical properties to the molecule, as wider HOMO-LUMO gap^{31,33,35-39}, and peculiar self-assembly behavior, favoring head-to-tail stacks at the solid state⁴⁰⁻⁴³ and vdW-driven assemblies on metal surfaces.⁴⁴ In this respect, borazines^{12,45} have recently renewed their interest as components for preparing optoelectronically-active materials⁴⁵⁻⁴⁷ and as precursors for preparing BN-doped graphitic nanostructures.^{48,49} The latest examples include the isolation of the first BN-doped coronene through pyrolysis^{50,51} and the synthesis of flower-like networks by surface-assisted polymerization.⁴⁹ However, due to the susceptibility of the BN core to undergo hydrolysis in the presence of moisture and the difficulty to prepare hybrid boron-nitrogen-carbon (BNC) materials with controlled doping patterns, the potential structural and optoelectronic diversity of borazine and its derivatives remain limited both in organic and materials chemistry.¹²

For their part, dendritic polyphenylenes conquered a pivotal role in nanoscience⁵²⁻⁵⁵ as shape-persistent nanoparticles, that depending on the peripheral chemical functions, could be used as UV emitters,⁵⁶ light-harvesting antennae,⁵⁷ and chemical precursors for the bottom-up synthesis^{58,59,4} of graphitic nanostructures. In view of these applications, hybrid polyphenylenes scaffoldings exposing borazine cycles placed in selected positions represent an unprecedented class of π -extended molecular boron-nitrogen-carbon (BNC) hybrid molecular materials. Further, it is expected that tuning the relative borazine orientation and the BN/C ratio one can tailor the materials properties. Given the emission properties⁴⁷ of hexaphenyl borazines and of their derivatives, it is anticipated that the replacement of the aromatic six-member rings with the BN-analogues will affect the optoelectronic properties of the polyphenylene skeleton. In this work we describe the preparation of the first hybrid BNC polyphenylenes featuring doping-dependent emissive properties.

General doping descriptors. Owing to the possibilities of introducing borazino units in different ratios, orientations, and positions, three different doping parameters should be considered when replacing benzene rings with the borazino analogues (Figure 1): the doping dosage (ρ); the doping orientation (\mathbf{o}), and the doping vector (\mathbf{d}_i). The doping dosage is defined as the percentage of the aryl units that have been substituted with the borazine analogues (Figure 1A). Instead, the orientational parameter \mathbf{o} defines the relative orientation between the doping borazine rings (Figure 1B). The \mathbf{o} descriptor is α when the relevant BN ring displays the same orientation as that of the reference borazine ring, otherwise β when rotated of 60° (Figure 1B). Finally, the doping vector \mathbf{d}_i describes the position of each doping units in a two-dimensional architecture following the X and Y coordinate axes originating from a reference BN ring defined as the (0,0) point (Figure 1C). Each coordinate is measured by the number of six-membered rings encountered along the two axes (y,x). Taken all together, the three descriptors ρ , \mathbf{d}_i and \mathbf{o} allow the precise depiction of the borazine-doping pattern of any

hybrid hexagonal polycyclic aromatic structure. Although not planar, polyphenylenes can be also looked as hexagonal structures if projected in a two-dimensional space; thus the very same doping descriptors can be used. In this first work, we will focus on the preparation of hybrid BNC polyphenylenes localizing doping borazine rings uniquely at the (0,0), (-10,5), (-5,-5), (5,-10), (10,-5), (-5,10) and/or (5,5) positions. To facilitate the reading, in this manuscript the (5,5), (5,-10) and (-10,5) doping positions are indicated as the *B*-sites, whereas the (-5,-5), (-5,10) and (10,-5) as the *N*-sites. Thus, a simplified nomenclature can be used in this paper: α_N (β_N or α_N) and α_B (β_B or α_B) when describing hybrid polyphenylenes bearing branching borazine units (with the 60° or 0° orientation, respectively) at the *N* and *B* positions of a given borazine reference.

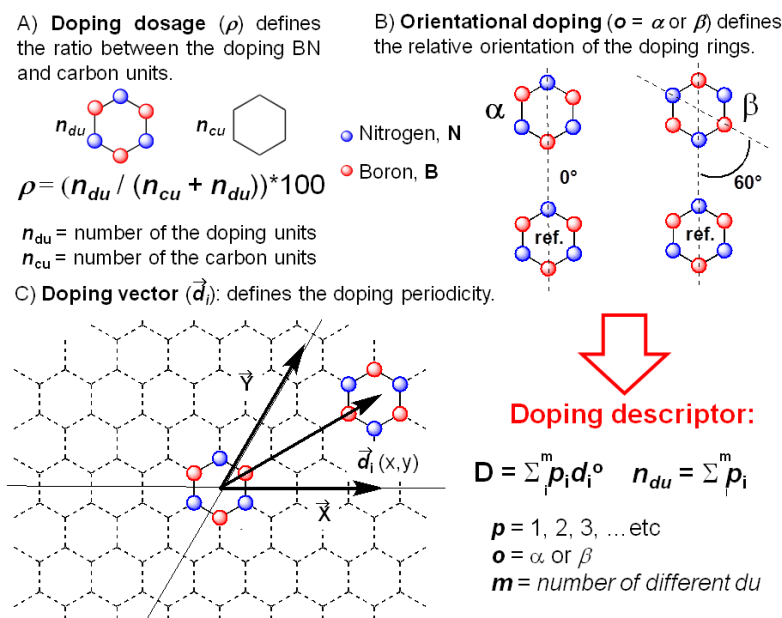


Figure 1. Parameters describing the doping pattern of borazino-doped hexagonal structures. Color code: blue: N, red: B.

Molecular design and divergent synthetic strategy. Considering that the borazine core can be made inert toward hydrolysis when aromatic substituents bearing *ortho* Me groups are connected to the *B* atoms,^{12,47,60} it can be inferred that Müllen's groundbreaking approach⁶¹ to prepare all-carbon polyphenylenes through cycloaddition reactions, would also lead to branched borazino-doped polyphenylene analogues. Indulging this synthetic protocol, we take advantage of the decarbonylative Diels-Alder cycloaddition reaction to divergently construct the first BNC polyphenylenes from reactive borazine modules that are alternatively functionalized with peripheral ethynyl or tetraphenylcyclopentadienone groups (Figure 2). Owing to the possibility of functionalizing the borazine core with different groups on the aryl substituents at the *N* and *B* atoms, we have envisaged to prepare borazino-doped polyphenylenes featuring different doping dosage ρ values and orientations α . To achieve it, two molecular modules were prepared: a core and a branching unit (Figure 2). The cores bear ethynyl moieties, whereas the branching units expose tetraphenylcyclopentadienone dienes. Depending on the chemical nature of the central aromatic module and of the reactive group, each covalent combination of the modules yields one exclusive doping pattern featuring controlled doping dosages and orientations.

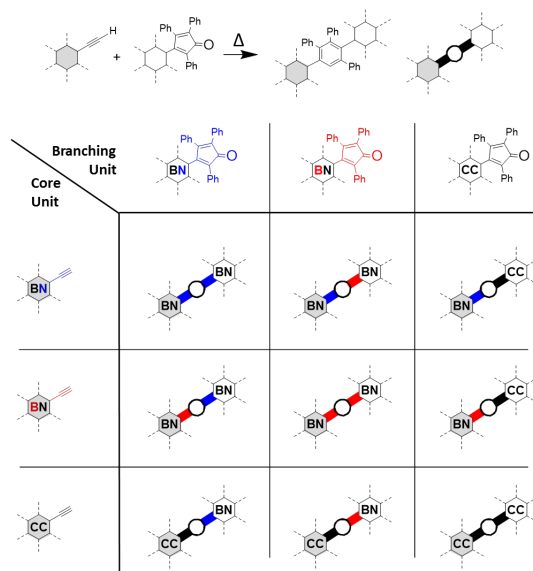
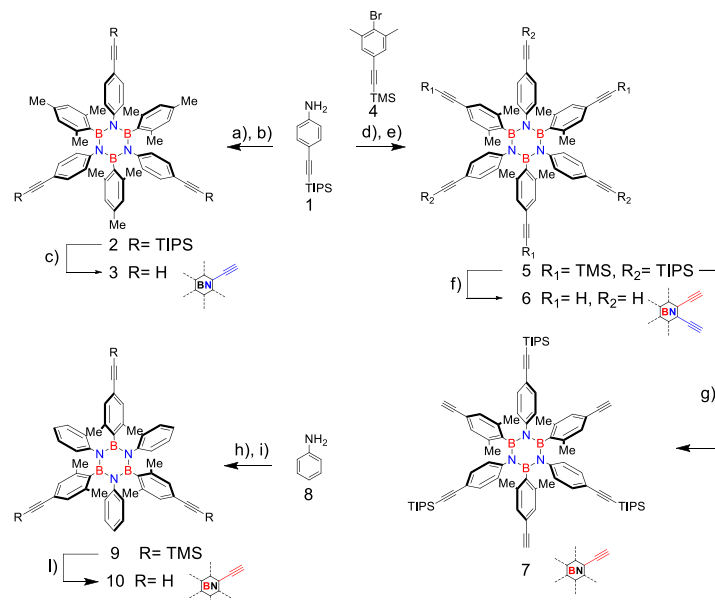


Figure 2. Envisaged doping patterns for the borazino-doped polyphenylenes investigated in this work. Color code: bleu, substituent at the N; red, substituent at the B.

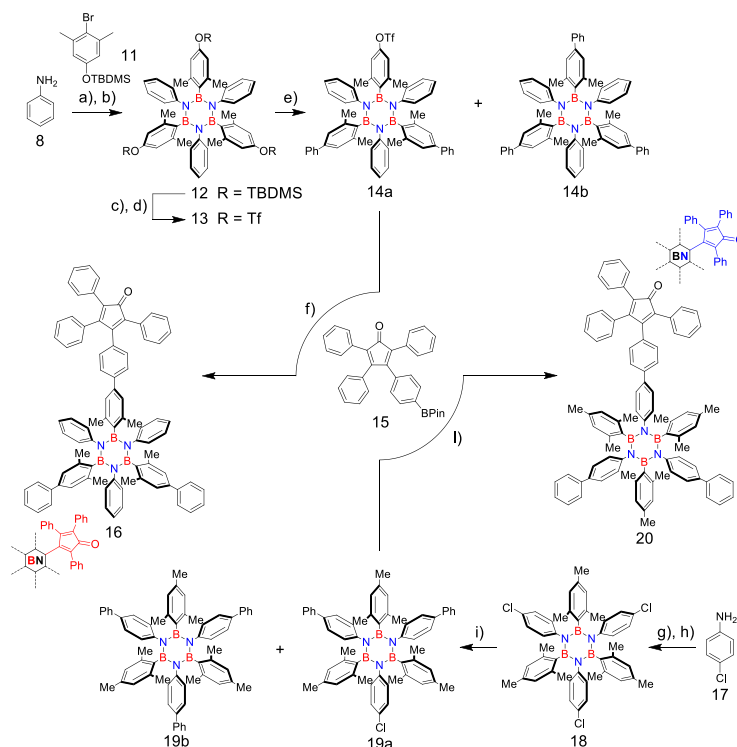
Results and Discussion

Synthesis of the borazine-derived ethynyl core modules. The borazine-derived cores used for the bottom-up synthesis of the borazino-polyphenylenes have been prepared following a modified protocol^{44,47,62} of the original *Groszos'* procedure.⁶³ For the core aryl-substituted borazine (Scheme 1) we started from TIPS-protected aniline **1** that was reacted with BCl_3 under refluxing conditions to give intermediate TIPS-protected *B*-trichloro-*N*-triphenylborazine. This, upon subsequent treatment with mesityllithium (MesLi) affords borazine core **2** in 54% yield (Scheme 1). Analogously, when intermediate TIPS-protected *B*-trichloro-*N*-triphenylborazine is reacted with the TMS-protected aryllithium derived from **4**, hexasilyl protected borazine core **5** could be prepared in 14% yield. Similarly, when *B*-trichloro-*N*-triphenylborazine is prepared from aniline, TMS-protected borazine core **9** could be also prepared upon addition of TMS-protected aryllithium derivative **4** in 34% yield. Removal of the silyl protecting groups of molecules **2** and **9** with TBAF yields borazines **3** and **10** exposing terminal phenylacetylene moieties at the *N*- and *B*-sites, respectively. As far as molecule **5** is concerned, addition of TBAF led to the full deprotection of the silyl groups, affording borazine core **6** exposing six terminal acetylene groups in 67% yield (Scheme 1). On the other hands, K_2CO_3 in MeOH allows the orthogonal removal of the TMS groups, thus affording tri-protected borazine core **7** in 69% yield (Scheme 1). Bearing three terminal ethynyl moieties at the boron centers, the latter borazine allows an orthogonal functionalization at the *N*- and *B*-sites (see below).



Scheme 1. Synthesis of borazino-based core modules: a) BCl_3 , toluene, reflux, 18 h; b) MesBr , $t\text{BuLi}$, THF, -84°C , 16 h, 54%; c) TBAF, THF, 0°C , 2 h, 77%; d) BCl_3 , toluene, reflux, 18 h; e) **13**, $t\text{BuLi}$, THF, -84°C , 16 h, 14%; f) TBAF, THF, 0°C , 2 h, 67%; g) K_2CO_3 , MeOH/THF (1:1), r.t., 16 h, 69%; h) BCl_3 , toluene, reflux, 24 h; i) **4**, $t\text{BuLi}$, THF, -84°C , 16 h, 34%; l) TBAF, THF, 0°C , 1 h, 96%. TBAF: tetrabutylammonium fluoride.

Synthesis of the borazine-derived tetraphenylcyclopentadienone branching modules. We conjectured that borazine-derived tetraphenylcyclopentadienones might be easily obtained from Suzuki cross-coupling reaction between an organoboron derivative of tetraphenylcyclopentadienone and a borazine exposing a suitable aryl halide or related electrophile (*i.e.*, ArOTf) either at the *N*- or *B*-sites.

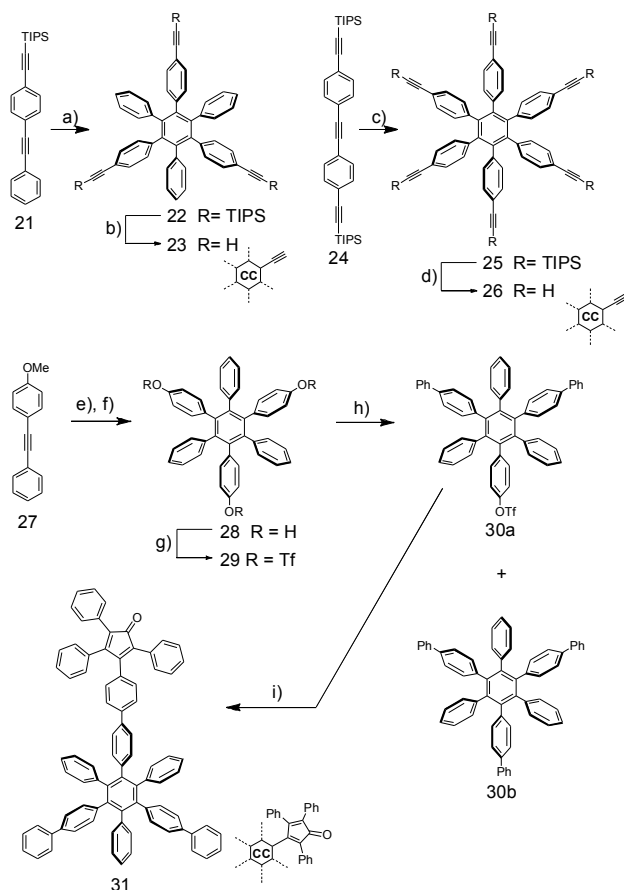


Scheme 2, above. Synthesis of borazine-derived cyclopenta-2,4-dienone branching module **16**: a) BCl_3 , toluene, reflux, 18 h; b) **11**, $t\text{BuLi}$, THF, -84°C , 2 h, 78%; c) TBAF, THF, 0°C , 2 h; d) Tf_2O , pyridine, r.t., 16 h, 78%; e) PhB(OH)_2 , $[\text{Pd}(\text{PPh}_3)_4]$, K_2CO_3 , dioxane/ H_2O (5:1), 105°C , 15 h, 39% (**14a**) and 8% (**14b**); f) **15**, $[\text{Pd}(\text{PPh}_3)_4]$, K_2CO_3 , dioxane/ H_2O (5:1), 105°C , 15 h, 71%. **Below.** Synthe-

sis of borazino-derived cyclopenta-2,4-dienone branching module **20**: g) BCl_3 , toluene, reflux, 18 h; h) MesBr, *t*BuLi, THF, $-84\text{ }^\circ\text{C}$, 2 h, 62%; i) $\text{PhB}(\text{OH})_2$, $[\text{Pd}_2(\text{dba})_3]$, K_3PO_4 , dioxane/ H_2O (5:1), $150\text{ }^\circ\text{C}$, 16 h, 27% (**19a**) and 25% (**19b**); l) **15**, $[\text{Pd}_2(\text{dba})_3]$, K_3PO_4 , dioxane/ H_2O (5:1), $150\text{ }^\circ\text{C}$, 20 h, 23%. Tf_2O : trifluoromethanesulfonic anhydride.

Thus, starting from aniline **8** (Scheme 2), we could synthesize TBDMS-protected borazine **12** as molecular precursor for preparing a suitable electrophilic partner to be reacted in the Suzuki cross-coupling reaction scheme. In particular, through the removal of the TBDMS protecting group with TBAF and successive esterification reaction with Tf_2O in pyridine, borazine **12** could be converted into tris-triflate borazine **13** in 78% yield. Suzuki cross-coupling between molecule **13** and phenylboronic acid (two equivalents), led to bis-phenyl and tris-phenyl borazine derivatives **14a** and **14b** in 39% and 8%, respectively (Scheme 2). Final cross-coupling reaction between monotriflate borazine **14a** and cyclopenta-2,4-dienone-derived boronic ester **15** gave targeted borazino-derived **16** in 71% yield. As we have anticipated potential vulnerability of the TBDMS protecting group under the acidic BCl_3 reaction conditions, a different synthetic strategy was undertaken for installing a suitable electrophile on the *N*-aryl group. Thus, a decision was made to equip the *N*-aryl substituent with a chloride functional group. Following these considerations, tris-chloride borazine **18** was firstly synthesized in 62% yield starting from 4-chloroaniline following the BCl_3 route (Scheme 2). Analogously to the case of borazines **14a** and **14b**, Suzuki cross-coupling reactions between phenylboronic acid (two equivalents) and borazine **18** led to bisphenyl and triphenyl derivatives **19b** and **19a** in 27% and 25% yield, respectively. Final grafting of cyclopenta-2,4-dienone-derived functionality occurred through a successive Suzuki cross-coupling reaction between boronic ester **15** and borazine monochloride **19a**, affording targeted molecule **20** bearing a cyclopenta-2,4-dienyl group on the *N*-aryl substituent.

Synthesis of the all-carbon core and branching modules. For the synthesis of the full-carbon modules, the Co-catalyzed cyclotrimerization strategy was used.⁶⁴ Whereas the cyclotrimerization of bis-TIPS-protected diphenylacetylene **24** in the presence of $\text{Co}_2(\text{CO})_8$ gave hexasubstituted benzene core **25** in 35% yield, the reaction with TIPS-protected diphenylacetylene **21** gave a mixture of two regioisomers (see ESI) that were separated by column chromatography yielding relevant hexaphenyl benzene **22** in 16% (Scheme 3). Removal of the TIPS group using TBAF gave tris-acetynyl hexaphenyl benzene **23** and hexaphenylacetynyl benzene **26** in very high yield. Regarding full-carbon branching unit **31**, a similar strategy to that undertaken for preparing core **23** was pursued. Specifically, cyclotrimerization of methoxydiphenylacetylene **27** in the presence of $\text{Co}_2(\text{CO})_8$ in dioxane followed by treatment with BBr_3 gave 1,3,5-tri-(4-hydroxy)-2,4,6-triphenylbenzene **28** in 14% yield. Reaction of **28** with Tf_2O in pyridine gave tri-triflate derivative **29** in 90% yield. Suzuki cross-coupling reaction between phenylboronic acid and **29** gave bis-phenyl and tris-phenyl derivatives **30a** and **30b** in 20% and 9% yield, respectively. Final Suzuki cross-coupling reaction between monotriflate **30a** and boronic ester **15** yielded full-carbon branching module **31** in 68% yield (Scheme 3).



Scheme 3, above. Synthesis of hexaphenylbenzene cores **22** and **25**: a) Co_2CO_8 , dioxane, reflux, 18 h, 16%; b) TBAF, THF, 0 °C, 3 h, 66%; c) Co_2CO_8 , dioxane, reflux, 48 h, 35%; d) TBAF, THF, 0 °C, 3 h, 96%. **Below.** Synthesis of hexaphenylbenzene-cyclopenta-2,4-dienone branching module **31**: e) Co_2CO_8 , dioxane, reflux, 18 h, f) BBR_3 , CH_2Cl_2 , -84 °C, 3 h, 14%; g) Tf_2O , pyridine, r.t., 18 h, 90%; h) $\text{PhB}(\text{OH})_2$, $[\text{Pd}(\text{PPh}_3)_4]$, K_2CO_3 , dioxane/ H_2O (5:1), 105 °C, 15 h, 20% (**30a**) and 9% (**30b**); i) **15**, $[\text{Pd}(\text{PPh}_3)_4]$, K_2CO_3 , dioxane/ H_2O (5:1), 105 °C, 15 h, 68%.

Synthesis of the three-branched borazino-doped polyphenylenes. To endorse the chosen synthetic plan, the thermal stability of the borazine core under the cycloaddition reaction conditions was first investigated. When molecule **3** is reacted with tetraphenylcyclopenta-2,4-dienone (CPD) in Ph_2O at 180 °C, borazino-oligophenylene molecule **32** decorated with three penta-phenylbenzene branches at the *N*-sites could be obtained in 56% (Scheme 4). To unambiguously prove the chemical structure, a small transparent crystal of **32**, suitable for X-ray diffraction, was obtained by solvent evaporation from a CHCl_3 solution. As expected, the X-ray molecular structure shows the presence of the penta-phenylbenzene peripheries at the *N* atoms of the borazine core (Figure 3). Given these premises, the synthesis of the different borazino-doped polyphenylenes was undertaken following the divergent covalent branching approach through decarbonylative [4+2] Diels-Alder cycloaddition reactions under heating conditions in Ph_2O containing the relevant core and branching units (Schemes 4-6). All molecules were purified through column chromatography and recycling gel permeation chromatography (Rec-GPC) using CHCl_3 as eluent. To commence, cycloaddition reaction between borazines **3** and **16** (Scheme 4) gave molecule **33** ($\rho = 8.9\%$) in which three peripheral borazine units are attached to the *N*-position of the central borazino core with a α_N orientational doping pattern.

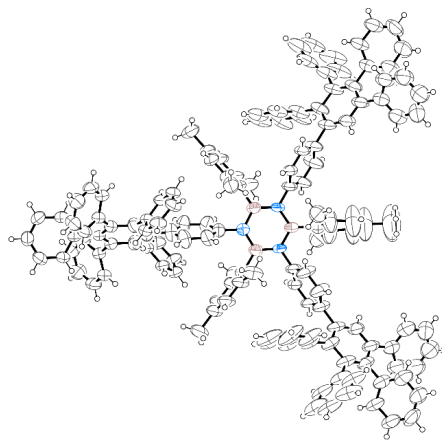
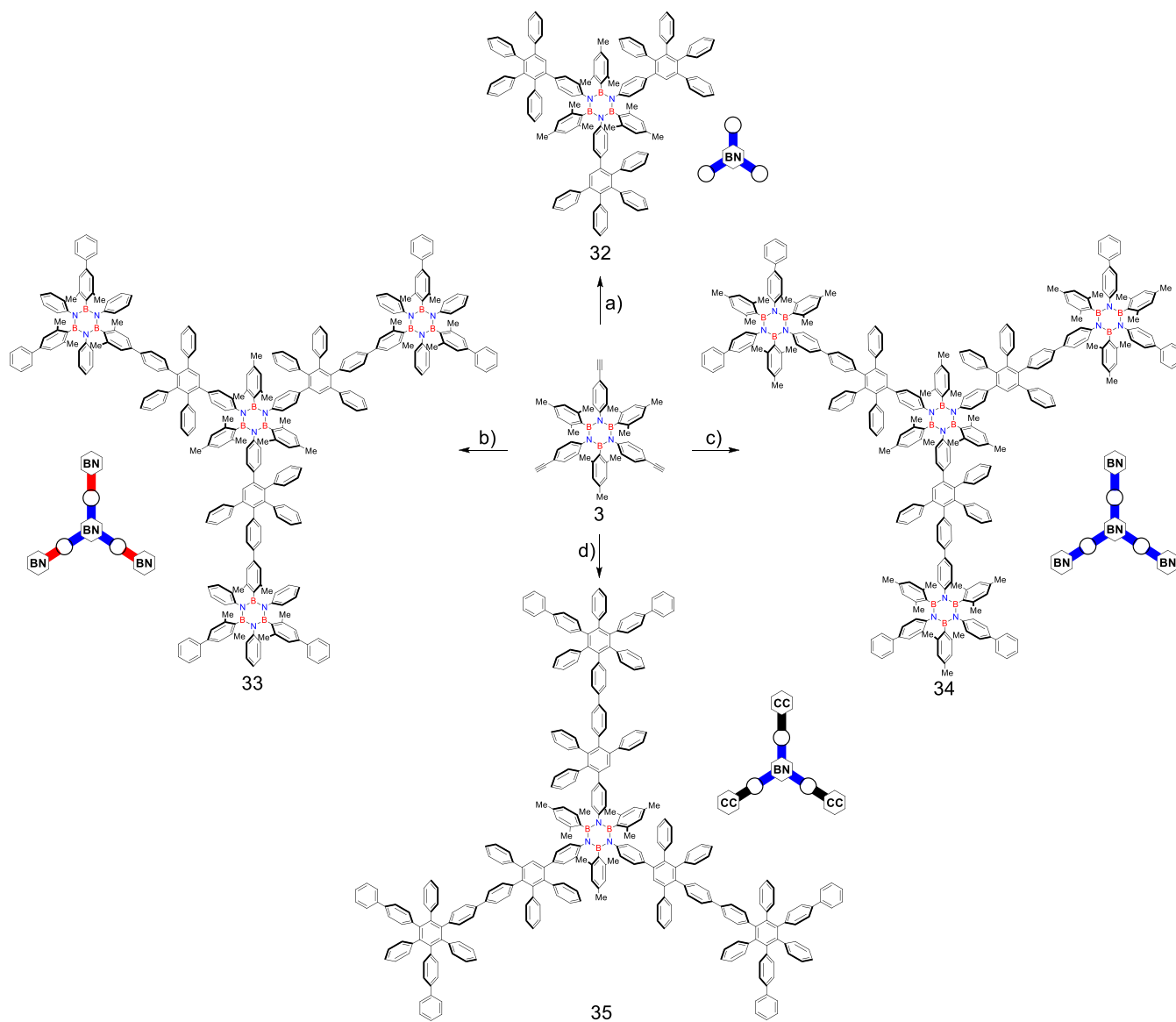
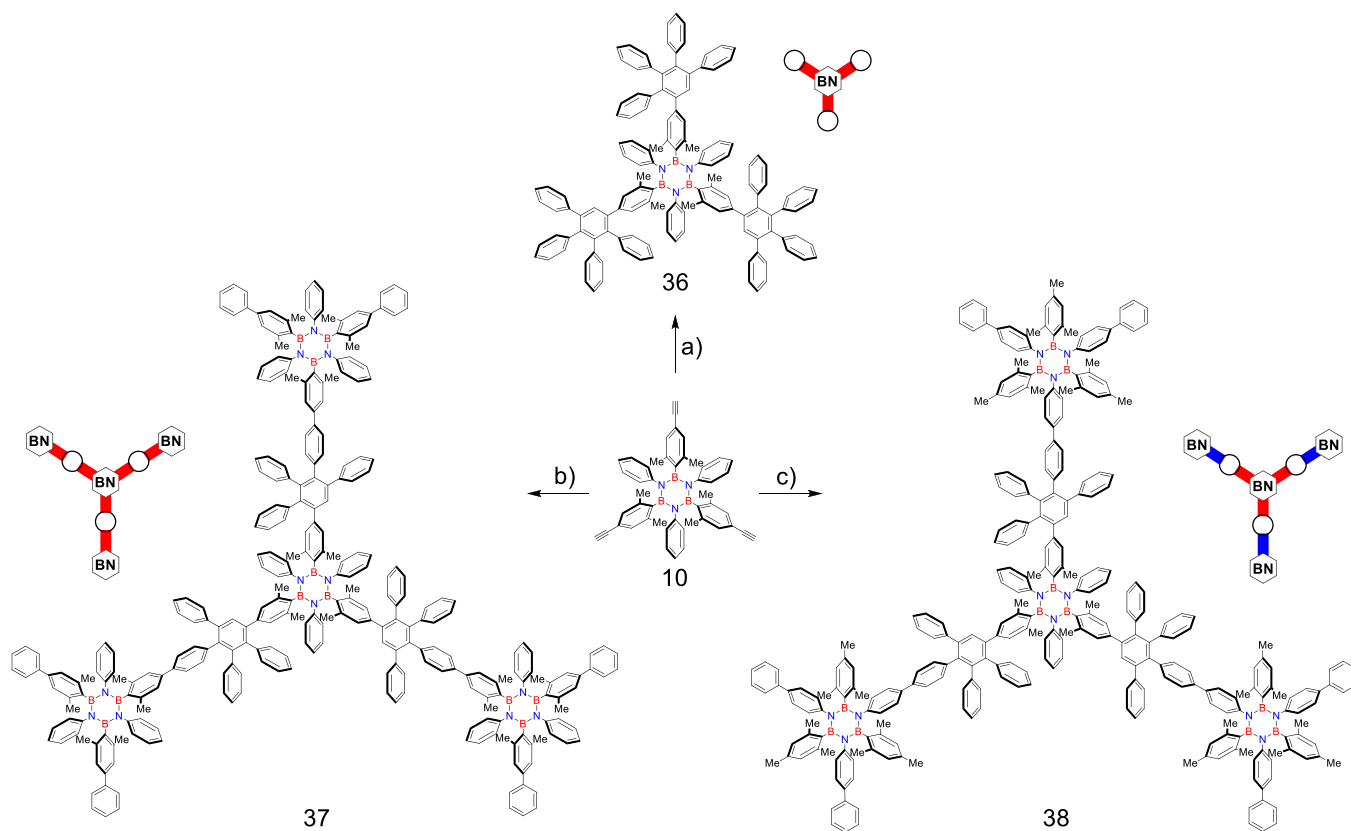


Fig. 3. ORTEP representation of borazine-polyphenylene **32** as determined by X-ray diffraction (atom colors: blue N, pink B, white C; atomic displacement parameters, obtained at 223 K, are drawn at the 50% probability level). Space group: $P2_1/c$. B-N bond lengths: 1.449; 1.451; 1.418; 1.444, 1.441 and 1.418 Å.

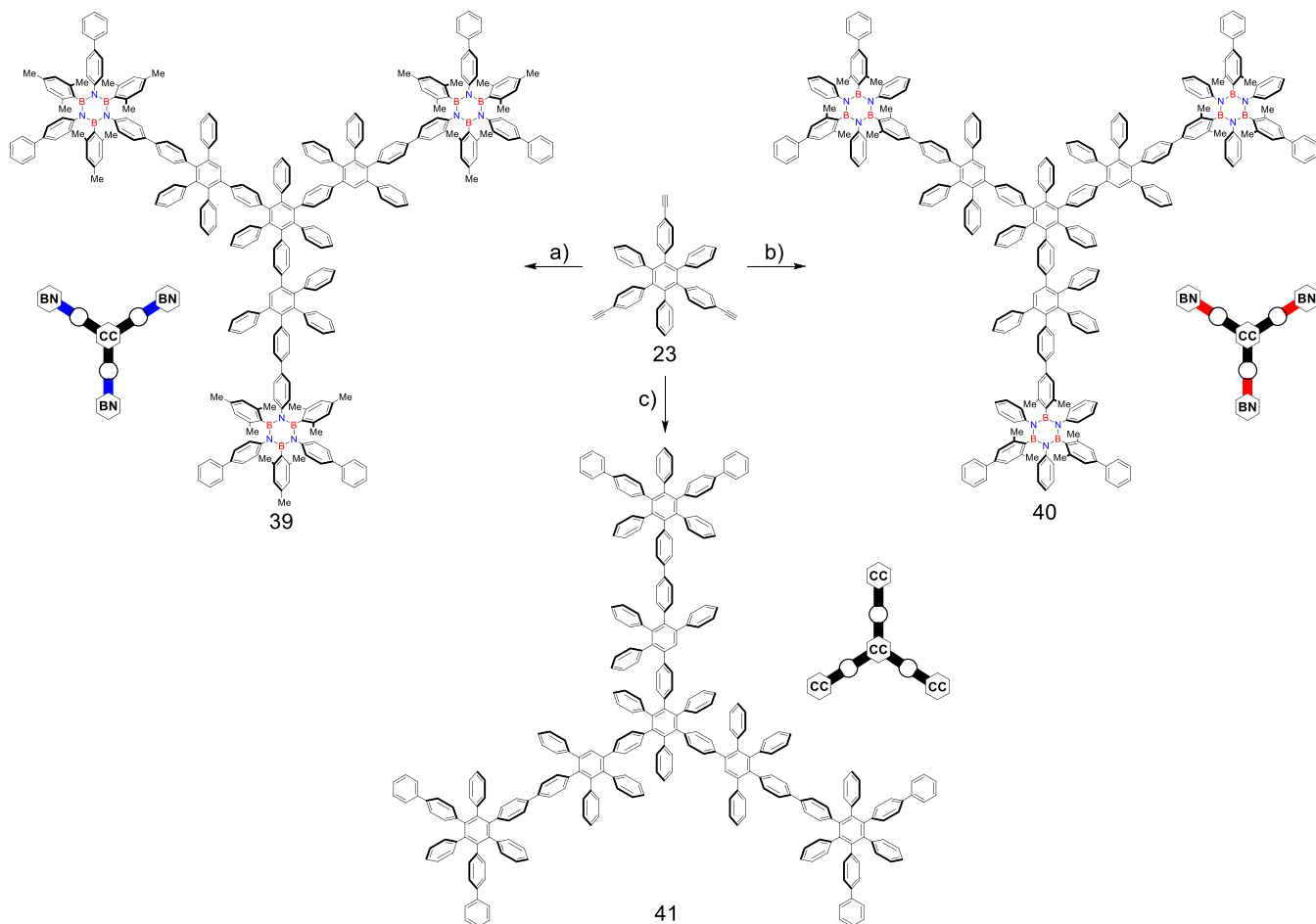


Scheme 4. Synthesis of borazine doped frameworks **32**, **33**, **34** and **35**: a) tetraphenylcyclopentadienone (CPD), Ph_2O , 180 °C, 2 h, 56%; b) **16**, Ph_2O , 180 °C, 18 h, 55%; c) **20**, Ph_2O , 200 °C, 16 h, 27%; d) **31**, Ph_2O , 190 °C, 18 h, 54%.

Following the same line, when borazine core **3** is reacted with cyclopenta-2,4-dienone **20**, branched borazylens **34** ($\rho = 8.9\%$) could be synthesized in 27%. Although the three peripheral borazine units are also attached to the *N*-position of central BN core, they are organized in a β_N orientational doping pattern. Finally, when borazine **3** is reacted with cyclopenta-2,4-dienone **31**, branched molecule **35** featuring low doping dosage ($\rho = 2.08\%$) with only a central doping borazine unit bearing all-carbon branches at the *N*-sites, is obtained in 54% yield. On the other hands, when borazine dienophile core **10** is used, branched hybrid polyphenylenes bearing the substituents exclusively at the *B*-sites could be prepared (e.g., *B*-branched penta-phenylbenzene reference borazine **36**). Capitalizing on this building block, cycloaddition reactions of core **10** with borazine dienes **16** and **20** (Scheme 5) gave branched borazylens **37** ($\rho = 8.9\%$) and **38** ($\rho = 8.9\%$) featuring β_B and α_B orientational doping patterns, respectively. In a similar manner, replacing the borazine core dienophile with full-carbon congener **23**, branched polyphenylenes **39** and **40** displaying an intermediate doping dosage ($\rho = 6.5\%$) and full-carbon reference **41** could be synthesized using dienes **20**, **16** and **31**, respectively (Scheme 6). Notably, branched polyphenylenes **39** and **40** develop the peripheral borazine units at the *N*- and *B*-site, all displaying α orientational doping pattern (i.e., α_N and α_B).

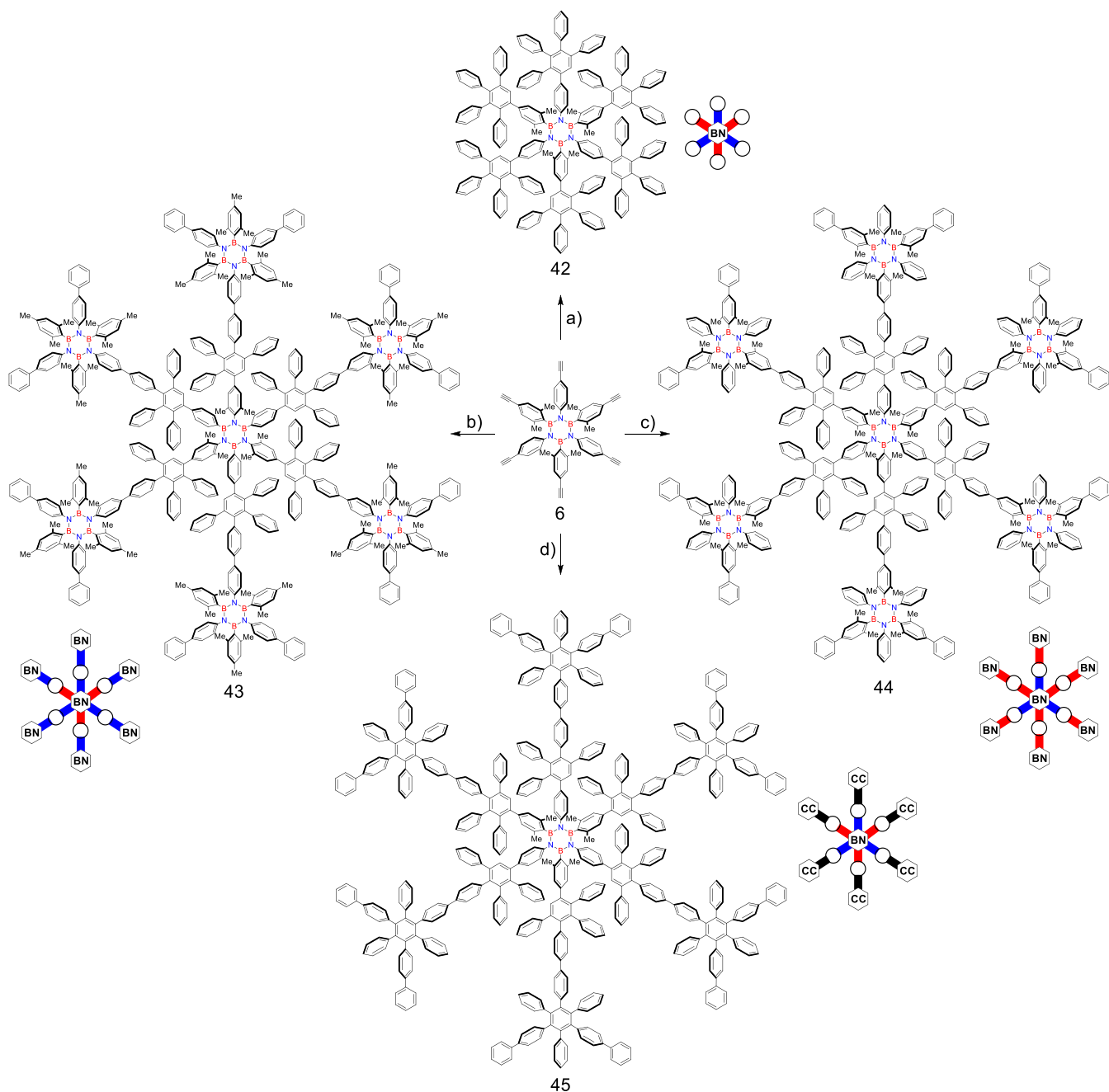


Scheme 5. Synthesis of borazine doped frameworks **36**, **37** and **38**: a) tetraphenylcyclopentadienone (CPD), Ph₂O, 180 °C, 6 h, 83% b) **16**, Ph₂O, 190 °C, 18 h, 22%; c) **20**, Ph₂O, 210 °C, 16 h, 40%.



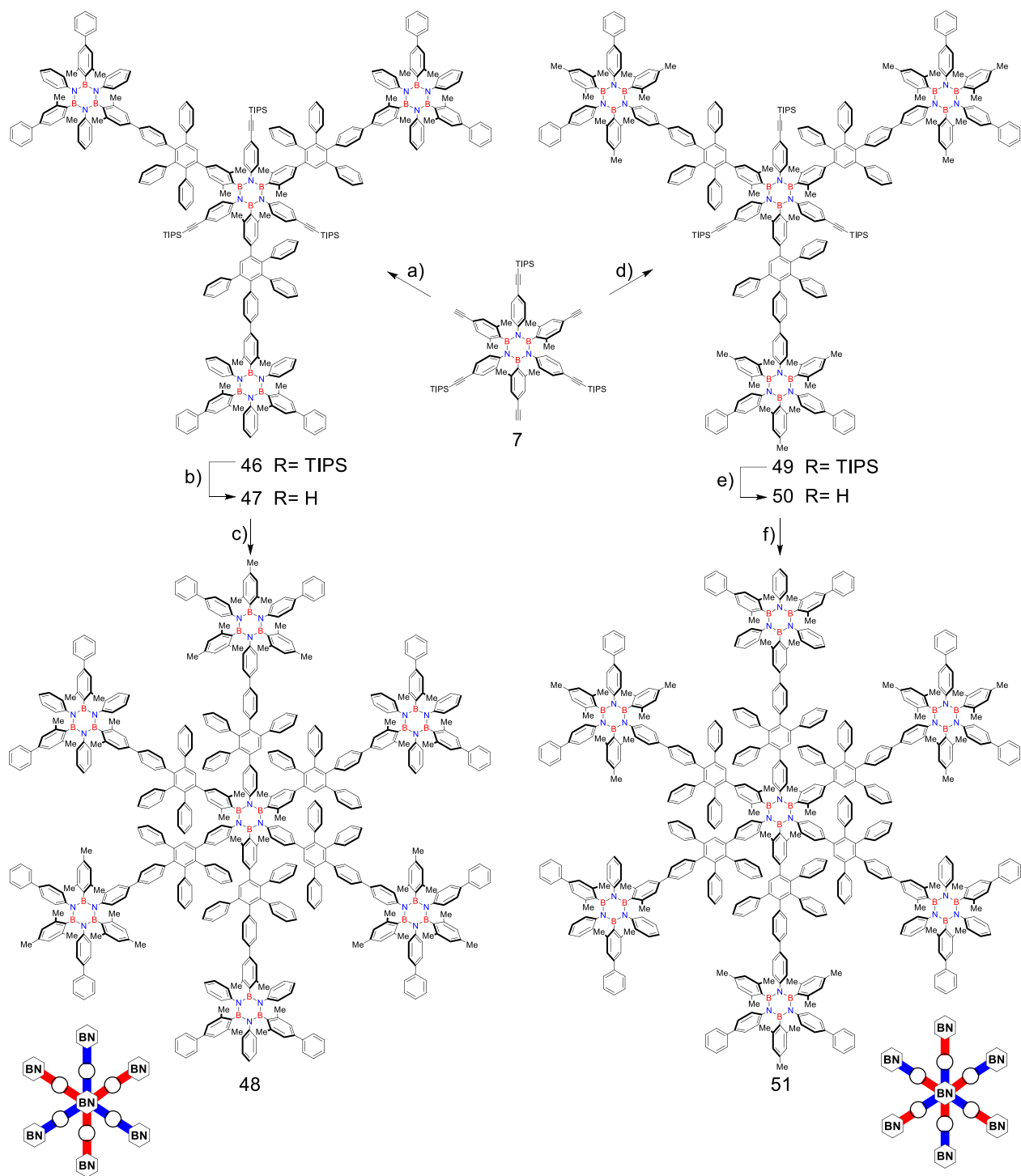
Scheme 6. Synthesis of borazine doped frameworks **39**, **40** and **41**: a) **20**, Ph₂O, 230 °C, 18 h, 27%; b) **16**, Ph₂O, 190 °C, 18 h, 81%; c) **31**, Ph₂O, 190 °C, 18 h, 51%.

Synthesis of the hexa-branched borazylenes. To extend further the number of borazine units within a polyphenylene architecture, hexa-branched derivatives were also prepared starting from the hexaethynyl borazine cores. As we have anticipated a potential steric hindrance deriving from the hexasubstitution at the hexa-substituted borazino core, the thermal conditions in Ph₂O of the cycloaddition reaction were first investigated using borazine core **6** in the presence of tetraphenylcyclopenta-2,4-dienone (CPD). As expected, borazino-oligophenylene **42** decorated with six pentaphenylbenzene branches could be obtained in good yield (48%) only when heated at least at 250 °C (Scheme 7). Following this plan, eight hybrid polyphenylenes displaying different doping dosage and orientations were prepared cross-reacting borazine dienophile cores **6**, **7**, **26** with branching dienes **16**, **20** and **31**. As discussed for the three-branched derivatives, also in this case the products were purified by column chromatography over silica followed by Rec-GPC using CHCl₃ as eluent.



Scheme 7. Synthesis of borazine-doped frameworks **42**, **43** ($\beta_N\alpha_B$), **44** ($\alpha_N\beta_B$) and **45**: a) tetraphenylcyclopentadienone, Ph_2O , 250°C , 16 h, 48% b) **20**, Ph_2O , 230°C , 16 h, 36%; c) **16**, Ph_2O , 260°C , 72 h, 35%; d) **31**, Ph_2O , 260°C , 30 h, 46%.

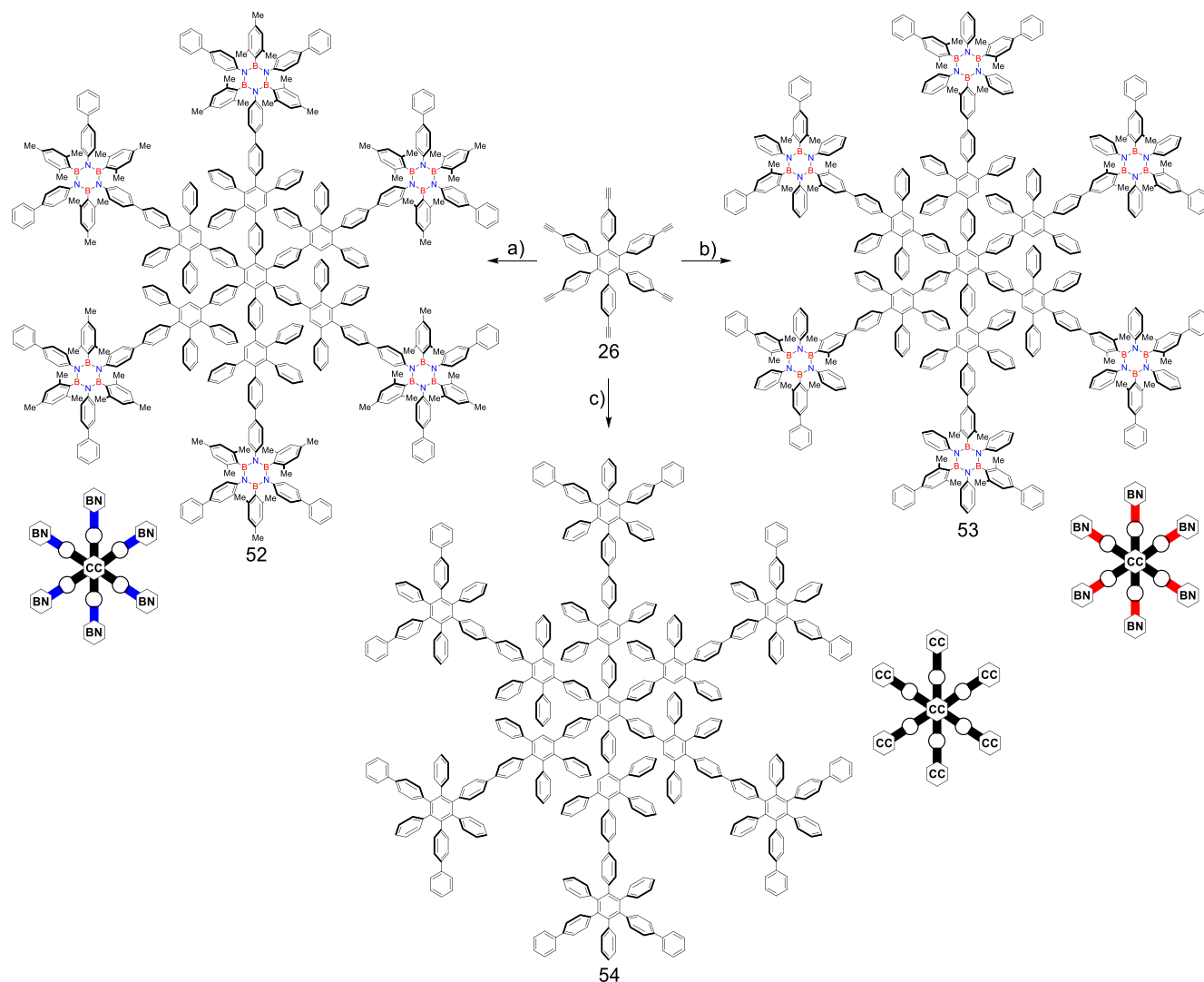
Specifically, when borazine core **6** is reacted with branching units **20**, **16** and **28**, hexa-branched polyphenylenes **43**, **44** and **45** were obtained in 36%, 35% and 46% yield, respectively (Scheme 7). Molecules **43** and **44** exposes seven borazine rings and displays the same doping dosage ($\rho = 8.33\%$) but orientational doping patterns $\beta_N\alpha_B$ and $\alpha_N\beta_B$, respectively. On the other hands, polyphenylene **45** only bears a central borazine unit, thus featuring low doping dosages ($\rho = 1.1\%$). Taking advantages of the orthogonal deprotection of the two silyl groups in molecule **5**, a stepwise [4+2] cycloaddition strategy was undertaken to prepare heptaborazine derivatives ($\rho = 8.33\%$) featuring $\beta_N\beta_B$ and $\alpha_N\alpha_B$ orientational doping patterns (Scheme 8).



Scheme 8. Synthesis of borazine doped frameworks **48** ($\beta_N\beta_B$) and **51** ($\alpha_N\alpha_B$): a) **16**, Ph_2O , 200°C , 18 h, 55%; b) TBAF, THF, 0°C , 2 h, 94%; c) **20**, Ph_2O , 260°C , 24 h, 54%; d) **20**, Ph_2O , 240°C , 18 h, 27%; e) TBAF, THF, r.t., 2 h, 84%; f) **16**, Ph_2O , 230°C , 16 h, 48%.

When triacetylene borazine core **7** is reacted with cyclo-2,4-dienone borazine **16**, tetraborazine intermediate **46** is obtained. Cleavage of the TIPS groups with TBAF followed by a second [4+2] cycloaddition reaction with diene **20**, gave targeted heptaborazine derivative **48** featuring a $\beta_N\beta_B$ doping pattern. Conversely, when inverting the cycloaddition reaction sequence, namely reacting dienophile **7** with diene **20** to give intermediate **50** followed by [4+2] cycloaddition with **16**, heptaborazine **51** ($\alpha_N\alpha_B$) was obtained. Replacing the borazine core

dienophile with corresponding full-carbon analogue **26**, branched hexaborazine polyphenylenes **52** and **53** displaying ρ value of 7.06% could be obtained (Scheme 9). As for the three-branched derivatives, branched polyphenylenes **52** and **53** develop the peripheral borazine units at the *N*- and *B*-site, all displaying α orientation (i.e., α_N and α_B). Finally, reference full-carbon polyphenylene **54** was prepared in 49% from hexaphenyl benzene core **26** and diene **31**.



Scheme 9. Synthesis of borazine doped frameworks **52**, **53** and **54**: a) **20**, Ph₂O, 230 °C, 16 h, 19% ; b) **16**, Ph₂O, 250 °C, 18 h, 70%; c) **31**, Ph₂O, 260 °C, 30 h, 49%.

The molecular structures of all cycloadducts were unambiguously identified by NMR spectroscopy (ESI) and mass spectrometry through the detection of the peak corresponding to the molecular ion (M^+). As examples, HRMS-MALDI mass spectrograms for **32** (C₁₃₅H₁₀₈B₃N₃⁺, calc.: 1803.8822, found: 1803.8802), **33** (C₂₉₇H₂₅₂B₁₂N₁₂⁺, calc.: 4118.1344, found: 4118.1251), **35** (C₂₉₇H₂₁₆B₃N₃⁺, calc.: 3856.7393, found: 3856.7273), **44** (C₅₄₆H₄₅₀B₂₁N₂₁⁺, calc.: 7532.8144, found: 7532.8324), and the MS-MALDI analysis for **53** (C₅₄₆H₄₃₈B₁₈N₁₈⁺, calc.: 7445.7, found: 7445.7), and **54** (C₅₄₆H₃₆₈⁺, calc.: 6926.9, found: 6926.8) are displayed in Figure 4.

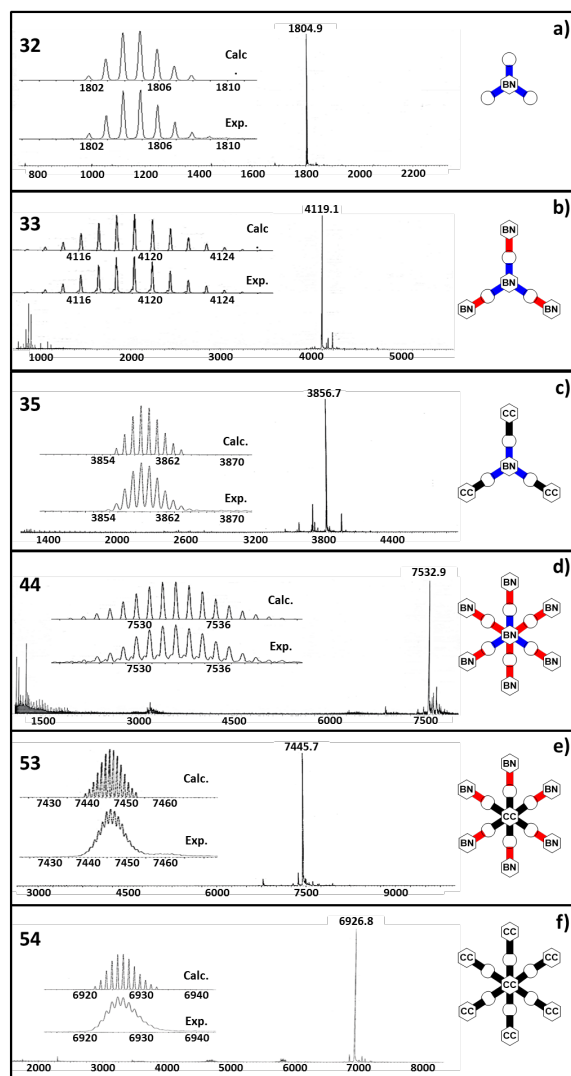
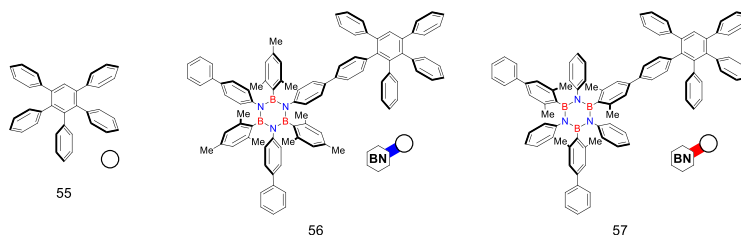


Fig. 4. Selected HRMS-MALDI mass analysis of **32** (a), **33** (b), **35** (c), and MS-MALDI mass analysis of **44** (d), **53** (e), and **54** (f) in the positive ion mode (matrix: DCTB, N_2 -laser: 337 nm). Insets: zoomed calculated (above) and experimental (below) spectra.



Scheme 10. Reference 1,2,3,4,5-pentaphenylbenzene **55**, and pentaphenylbenzyl borazines **56** and **57**.

For reference purposes, pentaphenyl benzene **55** and borazines **56** and **57**, bearing pentaphenylbenzene moieties respectively at the nitrogen and boron positions have been also synthesized (see ESI) by cycloaddition reaction between dienophiles **CPD**, **19a**, and **14a** with phenylacetylene, respectively.

Steady-state UV-vis absorption and emission studies in solution.

Comparative absorption spectra of the hybrid polyphenylenes in CH_2Cl_2 at 25 °C are shown in Figures 5 (see also ESI), with the key absorption data resumed in Table 1. In general, the absorption spectra for both three- and hexa-branched derivatives cover the UV spectral window in the ~200-325 nm range, as shown in Figure 5.

Both a broadening of the band and an enhancement of the UV-vis extinction coefficient (ϵ) at the maximum of absorption was observed upon increasing the number of borazine units (Figure 5): $\sim 6 \times 10^4$ for the reference borazine monomers, $1\text{-}3 \times 10^5$ for the three-branched derivatives and $3\text{-}6 \times 10^5$ for the hexa-branched conjugates (Table 1).

Table 1. Steady-state absorption and emission properties for the BN-doped and all-carbon polyphenylene derivatives in CH_2Cl_2 .

	Absorption		Emission						
	Comp. (ρ)	λ_{max} [nm] (ϵ , $\text{M}^{-1} \text{cm}^{-1}$)	λ_{exc} [nm]	λ_{max} [nm] (Φ_{em}) ^a	τ_{f} [ns] ^[b]	k_{f} [ns ⁻¹] ^[c]	$k_{\text{v}} + k_{\text{ISC}} + k_{\text{CS}}$ [ns ⁻¹] ^[d]	$\lambda_{\text{max}}^{77\text{K}}$ [nm]	$\lambda_{\text{max,PH}}^{77\text{K}}$ [nm]
MONO	30b (0%)	266 (7.1×10^4)	264	355 (9%)	0.3	0.3	3.03	344	-
	14b (1%)	269 (5.9×10^4)	263	327 (20%)	0.7	0.28	1.14	322	476, 451 ^e , 478 ^e , 505 ^e
	19b (1%)	267 (6.7×10^4)	273	322 (34%)	2.7	0.12	0.25	319	478
THREE BRANCHED	41 (0%)	268 (3.9×10^5)	274	372 (76%)	0.6	1.26	0.40	371	501, 423 ^e
	35 (2.08%)	266 (9.9×10^4)	279	373 (64%)	0.8	0.8	0.45	371	489, 432 ^e
	40 (6.5%)	267 (4×10^5)	266	373 (45%)	0.5	0.9	1.1	367	490, 406 ^e
	39 (6.5%)	268 (3.1×10^5)	272	373 (44%)	0.6	0.73	0.93	355	499
	33 (8.9%)	268 (1.7×10^5)	272	370 (33%)	0.5	0.66	1.34	365	484
	34 (8.9%)	265 (1.9×10^5)	272	370 (29%)	0.5	0.58	1.42	351	477
	38 (8.9%)	267 (2.7×10^4)	274	373 (11%)	0.2	0.55	4.45	362	508
	37 (8.9%)	269 (2.3×10^5)	275	372 (7%)	0.2	0.35	4.65	353	482
HEXABRANCHED	54 (0%)	266 (6.1×10^5)	280	376 (77%)	0.5	1.54	0.46	376	510, 423 ^e
	45 (1.1%)	265 (4.7×10^5)	268	372 (71%)	0.6	1.18	0.48	372	420, 504 ^e
	53 (7.06%)	269 (5.3×10^5)	263	370 (62%)	0.8	0.77	0.48	373	498, 423 ^e
	52 (7.06%)	267 (4×10^6)	266	375 (57%)	0.8	0.71	0.54	373	419
	44	263	275	374	0.8	0.32	0.93	365	521, 414 ^e

(8.33%)	(3.3×10 ⁵)		(26%)						
43	266	274	373	0.5	0.5	1.5	366	519, 420 ^e	
(8.33%)	(5.8×10 ⁵)		(25%)						
48	267	271	377	0.4	0.55	1.95	369	504, 402 ^e	
(8.33%)	(4.9×10 ⁵)		(22%)						
51	267	272	373	0.4	0.45	2.05	365	504, 417 ^e	
(8.33%)	(1.7×10 ⁵)		(18%)						

[a] Emission quantum yield (Φ_{em}); [b] life time at 295 nm; [c] radiative rate constant $k_r = \Phi_{em} / \tau_f$; [d] total no-radiative constant $(1/\tau_f) - k_r$; [e] shoulder phosphorescence peaks.

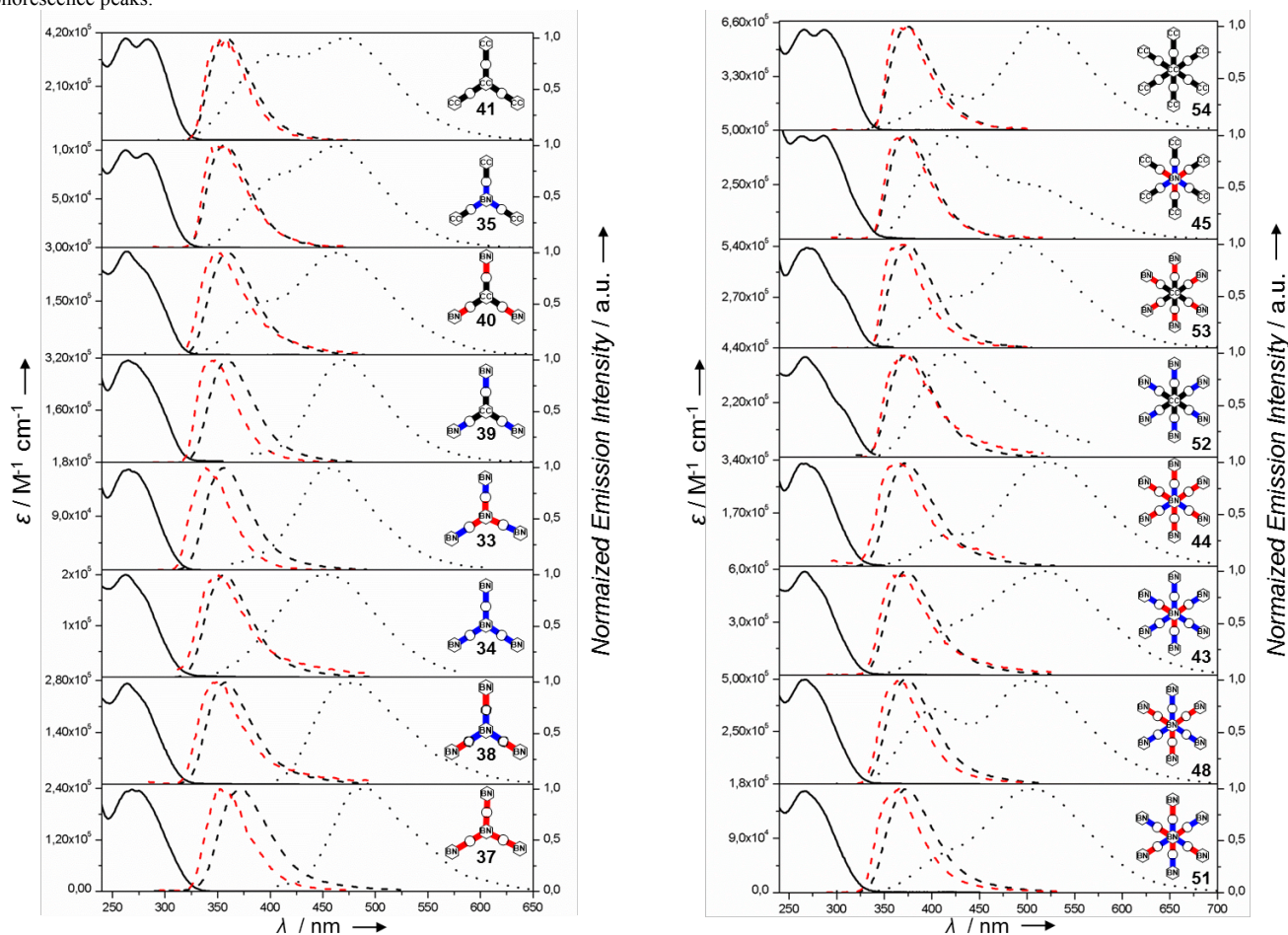


Figure 5. Absorption (—) at 298K, emission (---) at 298K, emission (---) at 77K, phosphorescence (...) at 77K spectra in CH₂Cl₂ of polyphenylenes (left) 33-41 and (right) 43-45, 48, 51-54.

While the highly doped polyphenylenes show a unique broad absorption bands, polyphenylenes with either low doping dosages or full-carbon content display a combination of two bands resulting in two peak maxima. Luminescence studies of air-equilibrated CH₂Cl₂ solutions of all borazine derivatives showed significant radiative UV emission profiles (centered in the interval between 263 and 280 nm) and very short lifetimes ($\tau = 0.4 - 0.8$ ns) consistent with the presence of excited singlet radiative deactivation. As expected, the excitation spectra fully match those of the corresponding absorption profiles confirming the all part of the molecules contribute to the emission. No significant changes in the emission profiles were observed at 77 K. All solutions showed

significant quantum yields (Φ_{em}), the intensity of which revealed to be dosage-dependent ($\Phi_{em} = 7\% - 76\%$; Table 1) for the branched derivatives, with the congeners displaying high doping dosages being the less emissive.

Monomeric structures and molecular references. Starting with reference borazine molecules **14b** and **19b**, one can notice that the presence of the phenyl substituents on the aryl rings linked to either the *N*- or *B*-sites clearly enhances the emission quantum yields ($\Phi_{em} = 20\%$ and 34% for borazines **14b** and **19b**, respectively) but reduces the life-time values ($\tau = 0.7$ ns and 2.7 ns for borazines **14b** and **19b**, respectively) if compared to the fluorescence intensity of *B*-trimesityl-*N*-triphenylborazine ($\Phi_{em} = 7.7\%$ and $\tau = 7.1$ ns in CH_2Cl_2).⁴⁷ In any circumstances, these monomeric borazine derivatives are stronger emitters than their all-carbon congeners, like molecule **30b** ($\Phi_{em} = 9\%$). The observed emission enhancement could be ascribed to the presence of the *ortho*-methyl groups that, hampering rotational movements, rigidifies the hexasubstituted borazine scaffold compared to that of hexaphenylbenzene derivatives. This consequently causes a decrease of the vibrational relaxation pathway. When branched, the emission intensity of the borazine scaffolds progressively diminishes upon increasing the number of the penta-phenylbenzene spokes ($\Phi_{em} = 20\%$, 16% , 2% and 0.8% for **56**, **57**, **32** and **36**, respectively, see Table 1S, ESI), with reference hexa-substituted penta-phenylbenzene borazine **42** being one of the least emissive of the series ($\Phi_{em} = 1\%$). Given the negligible emissive nature of the penta-phenylbenzene moieties ($\Phi_{em} < 1\%$ for **55**), the observed weakening of the emission intensity for all reference molecules can be realistically attributed to non-radiative vibrational deactivations triggered by the penta-phenylbenzene spokes. Notably, molecules bearing the functionalities exclusively at the *N*-sites are slightly more emissive than those functionalized at the *B*-sites (*i.e.*, $\Phi_{em}(\mathbf{19b}) > \Phi_{em}(\mathbf{14b})$; $\Phi_{em}(\mathbf{56}) > \Phi_{em}(\mathbf{57})$ and $\Phi_{em}(\mathbf{32}) > \Phi_{em}(\mathbf{36})$), suggesting that the functionalization pattern at the borazine core is not as innocent as one could think in the first place. In fact, being the observed double-bond character lower than 20% for the BN bonds (for *h*-BN the double bond character is $\sim 22\%$),⁶⁵ it can be considered that the *B* and *N* atoms are electrically neutral.⁶⁶ Thus, this suggests that each *N* atom retains the major electron bulges, while each *B* atom keeps their electronic deficiencies. This hypothesis is further confirmed by the calculated electron surface potential plots (ESPs, ESI), which show a charge polarization of the $\text{sp}^2\text{-B}_3\text{N}_3$ surface, with the *N* and *B* atoms negatively and positively charged, respectively. As previously reported for boron-nitrogen containing donor acceptor dendrimers,⁶⁷⁻⁷⁰ photoinduced short-living charge separated (CS) states undergoing dynamic processes could take place between electron-donating and electron-accepting moieties, deactivating the emissive excited states.

Three-branched polyphenylenes. Moving to the three-branched polyphenylene series, one can appreciate a significant decrease of the emission intensity when increasing the doping dosage (Table 1, Figure 6). The fluorescence quantum yield of the all-carbon polyphenylene is measured as the strongest value (76%), whereas the progressive replacement of aryl rings with B_3N_3 surprisingly lessens the emission intensities (Figure 6),

with the tetraborazine derivatives being the weakest emitters.

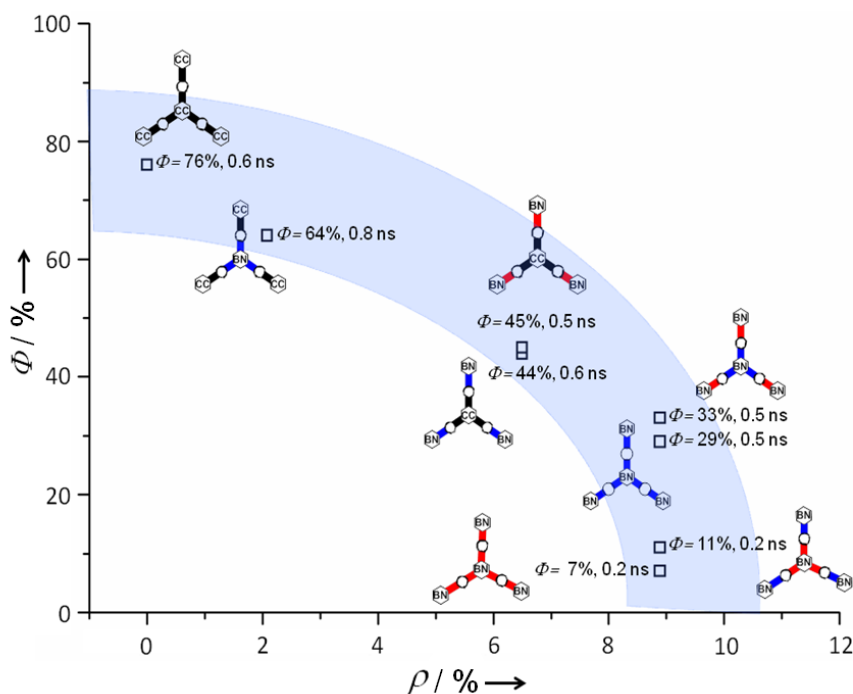


Figure 6. Emission quantum yield as a function of the dosage and orientational doping for the three-branched polyphenylenes series.

This behavior is rather unexpected if one considers that monomeric borazine molecules **14b** and **19b** are more emissive compared to their hexaphenylbenzene analogue **30b**.⁴⁷ The observed emission enhancement for molecule **35** could be reasonably attributed to an overcrowding effect that, generated by the simultaneous presence of multiple branching units,^{56,71-74} rigidifies the dendritic structure and enhances the emission intensity as previously observed with other full carbon polyphenylenes.⁷⁵ Interestingly, while the insertion of the B₃N₃ ring at the (o,o) position seems to have a minor effect on the emissive properties ($\Phi_{em} = 67\%$ for **35**), a significant decrease of the fluorescence intensity is obtained when borazine units are present at the periphery ($\Phi_{em} = \sim 45\%$ for both **39** and **40**). Notably, no effects of the borazine *N*- or *B*-site is observed for molecules **39** and **40**, as both conjugates essentially display the same Φ_{em} values. As anticipated above, the major fluorescence quenching is observed for the four tetra-borazine derivatives ($\Phi_{em} < 33\%$), bearing both inner and peripheral borazine rings. Among those, molecules **37** and **33** featuring β_B and α_B orientational doping patterns display the weakest emissions ($\Phi_{em} = 7\%$ and 11% , respectively), whereas derivatives **34** and **38** display the highest values ($\Phi_{em} = 29\%$ and 33% , respectively). When the measurements are performed in O₂-free solutions, the Φ_{em} values are essentially the same as those measured in air-equilibrated solutions. Calculation of the radiative (k_f) and total non radiative ($k_{nr} = k_v + k_{ISC} + k_{CS}$) rate constants (Table 1) allowed us to shed further light on the effect of the doping on the deactivation pathways. As it clearly appears from the derived rate constants values, increasing the BN dosages accelerate a non-radiative deactivation rate of the singlet-excited state through a possible combination of ISC, increase of the CS character of the excited states and vibrational relaxation. Among all, we can reasonably consider that the ISC and photoinduced CT are the most contributing pathways given the emissive behavior of the dendritic structures compared to that of molecular references **32**, **36**, **55-57**.

The quenching of the emission is particularly high when the peripheral borazines branches out through the *B*-sites (*i.e.*, molecule **37**). A total non-radiative deactivation 12 times faster than that of the full-carbon analogue was observed. When cooled to 77 K, non-negligible phosphorescence emission have been observed (Figure 5) showing double-peak emission profiles, with the borazine-doped molecules generally featuring the highest-energy triplet emission (Table 1), in line with previously-studied BN-containing polycyclic aromatics.⁴¹ Representative phosphorescence lifetime measurements (Figure 188S) showed long-lasting emission profiles ($\tau_{\text{Phos}} = 2.6, 2.1$ and ~ 2 s for **14b**, **36**, **33**) for the borazine-containing derivatives compared to that ($\tau_{\text{Phos}} = 1.1$ s for **41**) of the full carbon analogues.

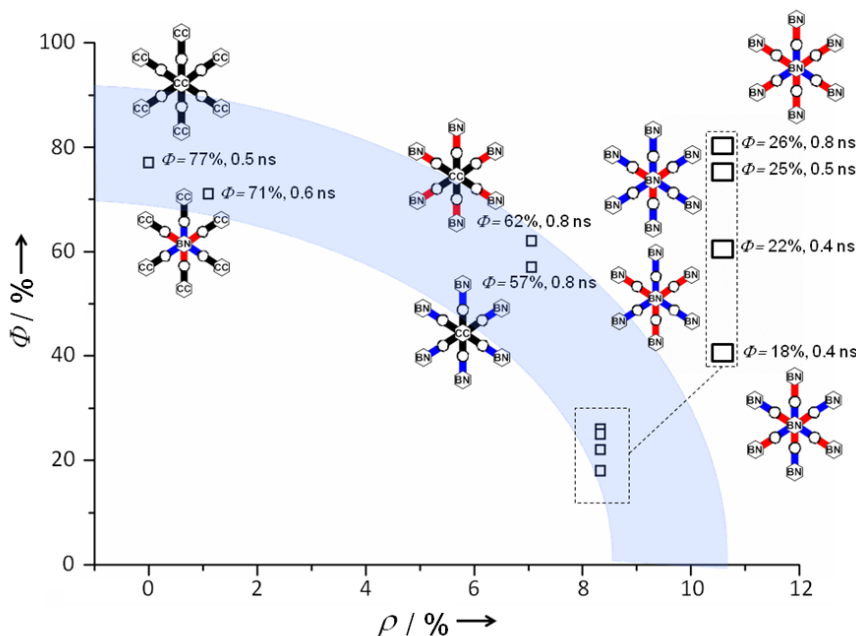


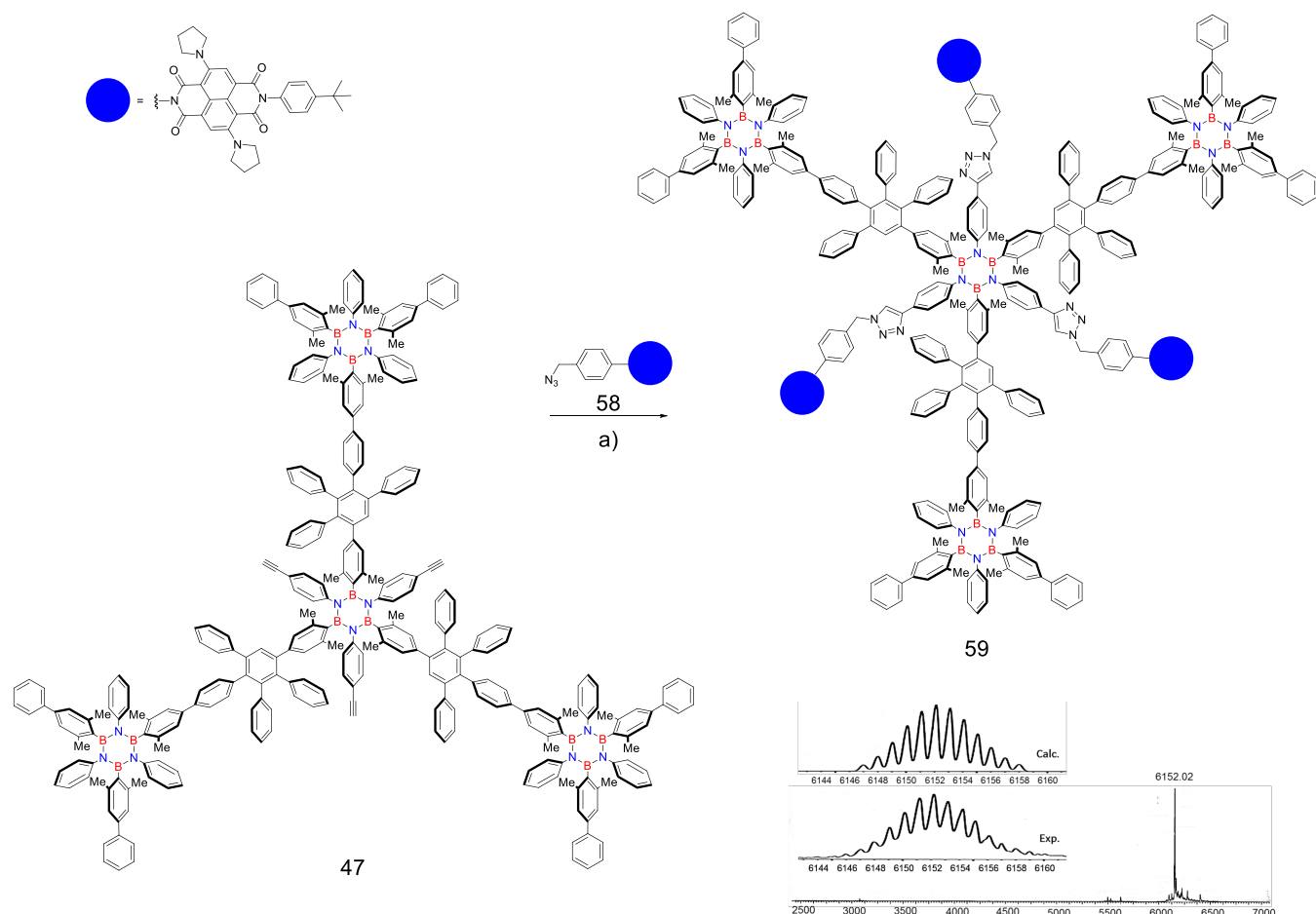
Figure 7. Emission quantum yield as a function of the dosage and orientational doping for the hexa-branched polyphenylenes series.

Hexa-branched polyphenylenes. Similarly to the three-branched polyphenylenes, also the hexa-branched polyphenylenes show a clear decrease of the emission intensity upon increasing the doping dosage (Table 1, Figure 7). With the all-carbon polyphenylene **54** showing the strongest emission (77%), the replacement of either the central or the six aryl rings with the B_3N_3 analogues causes a modest quenching of the emission intensities, with hexaborazino derivatives **52** and **53** being the weakest fluorophores (57%-62%). As observed for the three-branched architecture, only the simultaneous presence of the central and peripheral borazine units (*i.e.*, heptaborazino derivatives **43**, **44**, **48** and **51**) provokes a significant quenching of the fluorescence signal (18%-26%). In contrast to the tetraborazino architectures, in this case no significant effect of the orientational doping was observed for the heptaborazino derivatives, with the four patterns $\alpha_N\alpha_B$, $\beta_N\alpha_B$, $\alpha_N\beta_B$, and $\beta_N\beta_B$ displaying very similar Φ_{em} values. Together with the calculated radiative and total deactivation rate constants (Table 1), these data further advocate the observation for which increasing BN dosages enhance the deactivation rate of the singlet excited state of these BNC polyphenylenes. However, at these high dosages negligible effect on the emission intensities was observed when changing the orientation of the doping units. This sug-

gests that the σ_N/σ_B parameter does not play a major role in affecting the excited states when the BNC polyphenylenes features high ρ ratios. Probably, at high doping dosages, multiple electronic interactions take place in the hybrid BNC polyphenylene averaging the emission intensity. As observed for the three-branched derivatives, also the hexa-branched polyphenylenes present non-negligible a two-peak phosphorescence emission profile at 77 K.

Synthesis of a multichromophoric BNC polyphenylene.

To further probe the energy harvesting properties of BNC polyphenylenes, a multichromophoric derivative constituted by a tetra-borazino polyphenylene β_B architecture interring a red-absorbing dye at its central core has been synthesized (Scheme 11). The blue naphthalene diimide (B-NDI) tag^{76,77} was selected for its complementary lowest-energy UV-Vis absorption profile that, covering the red region, does not overlap with that of the tetraborazino-doped framework (TBOZ). Taking advantages of the orthogonal cleavage of the protecting silyl groups in molecule **5**, we have decided to further enrich the reactivity portfolio pertinent to the borazine core attempting a Cu-catalyzed 1,3-dipolar cycloaddition reaction to give a triazole unit (Scheme 11).



Scheme 11. Synthesis of NDI-bearing tetraborazine **59**: a) **58**, DIPEA, AcOH, CuI, CH₂Cl₂, r.t., 96 h, 58%.

Starting from triethynyl tetraborazine intermediate **47** (Scheme 8), and subjecting it to Cu-catalyzed 1,3-dipolar cycloaddition with an azido-derived naphthalene diimide chromophore **58** (see ESI for the

synthesis),⁷⁸ blue-colored tetraborazine polyphenylene **59** was obtained. Despite the presence of the resident oligophenylenes branches, remarkable high yields were obtained for the cycloaddition and no decomposition of the borazine core was observed under the given Cu-catalyzed reaction conditions. Once again, the product was purified by silica gel chromatography and recycling GPC (RGPC, see ESI). The molecular structure was unambiguously identified by HR-MALDI through the detection of the peak corresponding to the molecular ion (M^+) at m/z 6152.02 ($C_{417}H_{357}B_{12}N_{33}^+$, calc.: 6151.97; see ESI). Similarly to the other BNC polyphenylenes, we have evaluated the steady-state absorption and emission properties of molecule **59**. The dyad mainly absorbs in two regions with distinct peaks at 603, 364, 347, 262 nm, characteristic of the TBOZ framework and of the B-NDI unit, respectively (Figure 8). By choosing $\lambda_{exc} = 272$ nm, it was possible to predominantly excite (74%, according to the extinction coefficient of the model compounds) the tetraborazylene unit. At $\lambda_{exc} = 272$ nm, the emission spectra of the TBOZ moiety is essentially quenched ($\approx 98\%$) in CH_2Cl_2 (residual $\Phi_{em}^{BOZ} = 1.98\%$ at $\lambda_{em} = 357$ nm, see ESI).

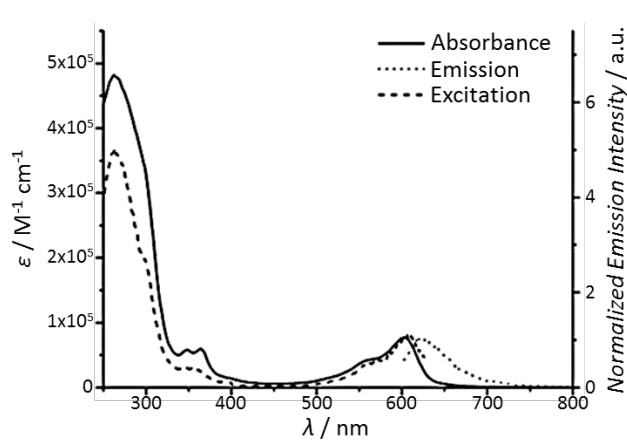


Figure 8. Extinction coefficient (—, $\epsilon_{max} = 4.8 \times 10^5 \text{ L mol}^{-1} \text{ cm}^{-1}$ at $\lambda = 262$ nm), emission (⋯, $\lambda_{exc} = 263$ nm) and excitation profiles (---, $\lambda_{em} = 650$ nm) of blue-labelled **59** in CH_2Cl_2 at 25 °C.

However, a B-NDI-centered luminescence is clearly visible, with a Φ_{em}^{B-NDI} value of $\sim 0.5\%$. Given the low values and the experimental error, the Φ_{em} is virtually the same to that of the NDI model compound obtained upon direct excitation (at $\lambda_{exc} = 560$ nm). This suggests that the photophysical behavior of the NDI chromophores is not affected by the burying borazino-doped polyphenylene architecture. The excitation spectrum of **59** (Figure 8) further supported the ET hypothesis, showing a strong contribution of the TBOZ scaffold to the emission of the lowest-energy acceptor B-NDI. The energy transfer efficiency (Φ_{ET}) has been estimated following the method by Melinger *et al.*⁷⁹ In particular, by using the equation $\Phi_{ET} = E_{TBOZ}^c / A_{TBOZ}^c$, where E_{TBOZ} and A_{TBOZ} are fluorescence intensity and absorption of the donor TBOZ scaffold corrected by residual absorption of the NDI moiety (see ESI), a remarkable energy transfer efficiency of 83% has been estimated ($\lambda_{exc} = 262$ nm). This suggests the presence of a fast energy transfer (ET) process leading to an efficient TBOZ→B-NDI sensitization. Taken all together, these data advocate these BNC hybrids suitable antenna systems, as previously extensively documented for the all-carbon analogues developed by Müllen and co-workers.^{80–82}

Conclusions

In conclusion, in this paper we have reported the first example about the use of borazine as a versatile modular building blocks to prepare hybrid BNC polyphenylenes featuring doping borazino cores at selected positions, given ratios and orientation patterns. Owing to the possibility of functionalizing the borazine core with different groups on the aryl substituents at the *N* and *B* atoms, we have prepared BNC polyphenylenes taking advantage of the decarbonylative [4+2] Diels-Alder cycloaddition reaction. To achieve it, two molecular modules were prepared: a core and a branching unit. Depending on the chemical nature of the central aromatic module and of the reactive group, each covalent combination of the modules could yield one exclusive doping pattern. As far as the borazine building blocks are concerned, di-*ortho*-methyl substituted aryl moieties were used to protect the electrophilic boron atoms. Indulging this approach, we have prepared the first three- and hexa-branched hybrid polyphenylenes featuring controlled orientation and dosages of the doping B₃N₃-rings. Detailed photophysical investigations, showed that upon increasing the doping dosage, the strong luminescent signal is progressively reduced ($\Phi_{em} = 76\% - 7\%$). This observation suggests that the presence of B₃N₃-rings possibly increase the CS character of the excited states favouring a non-radiative deactivation of the singlet-excited states. Notably, the effect of the borazine substitution pattern on the emission quantum yields was only observed for those hybrid BNC polyphenylenes featuring low doping dosages. To further probe the energy harvesting properties and chemical versatility of BNC polyphenylenes, a multichromophoric derivative constituted by a tetra-borazino polyphenylene bearing three blue-colored dyes was also prepared through Cu-catalyzed 1,3-dipolar cycloaddition.

Taken all together, these results suggest that sterically-protected borazines can be used as versatile aromatic platforms just like benzene and its derivatives. The ability of acquire 'at-will' substitution and doping patterns, make these BNC polyphenylene architectures versatile molecular precursors for synthesizing planarized graphitic nanostructures featuring controlled doping patterns. However, the lack of a suitable planarization protocol allowing the formation of C-C bonds in the presence of BN-type aromatics still limits the bottom-up approach for the preparation of regularly BN-doped molecular graphenes. This will be the synthetic challenge of our future endeavors in the molecular BNC field.

ASSOCIATED CONTENT

Supporting Information

Synthetic protocols and spectroscopic characterisations. This material is available free of charge via the Internet at <http://pubs.acs.org>.

AUTHOR INFORMATION

Corresponding Author

bonifazid@cardiff.ac.uk

Author Contributions

‡These authors contributed equally.

Notes

The authors declare no competing financial interest.

ACKNOWLEDGEMENT

D.B. gratefully acknowledges the FRS-FNRS (FRFC contract n° 2.4.550.09), the Wallon Region for the 'Flycoat' and 'TUBOLED' POC projects, the Science Policy Office of the Belgian Federal Government (BELSPO-IAP 7/05 project). We thank the ETHZ mass service for the HR-MALDI measurements for compounds **33** and **44**. We thank Dr. Andrea Fermi (Cardiff University) for the help in recording the life-time values and interpreting the photophysical characterization. We thank Mr. Nicolas Biot (Cardiff University) for the plotting of the ESP surface potential.

REFERENCES

- (1) Wang, X.; Sun, G.; Routh, P.; Kim, D. D.-H.; Huang, W.; Chen, P. *Chem. Soc. Rev.* **2014**, *43*, 7067–7098.
- (2) Stępień, M.; Gońka, E.; Żyła, M.; Sprutta, N. *Chem. Rev.* **2017**, *117*, 3479–3716.
- (3) Baumgartner, T. *Acc. Chem. Res.* **2014**, *47*, 1613–1622.
- (4) Narita, A.; Wang, X.-Y. X.; Feng, X.; Müllen, K. *Chem. Soc. Rev.* **2015**, *44*, 6616–6643.
- (5) Liu, Z.; Marder, T. B. *Angew. Chem., Int. Ed.* **2008**, *47*, 242–244.
- (6) Wang, X.-Y.; Wang, J.-Y.; Pei, J. *Chem. Eur. J.* **2015**, *21*, 3528–3539.
- (7) Bosdet, M. J. D.; Piers, W. E. *Can. J. Chem.* **2009**, *87*, 8–29.
- (8) Numano, M.; Nagami, N.; Nakatsuka, S.; Katayama, T.; Nakajima, K.; Tatsumi, S.; Yasuda, N.; Hatakeyama, T. *Chem. Eur. J.* **2016**, *22*, 11574–11577.
- (9) Wang, X.; Zhang, F.; Schellhammer, K. S.; Machata, P.; Ortmann, F.; Cuniberti, G.; Fu, Y.; Hunger, J.; Tang, R.; Popov, A. A.; Berger, R.; Müllen, K.; Feng, X. *J. Am. Chem. Soc.* **2016**, *138*, 11606–11615.
- (10) Golberg, D.; Bando, Y.; Huang, Y.; Terao, T.; Mitome, M.; Tang, C.; Zhi, C. *ACS Nano* **2010**, *4*, 2979–2993.
- (11) Campbell, P. G.; Marwitz, A. J. V.; Liu, S.-Y. *Angew. Chem., Int. Ed.* **2012**, *51*, 6074–6092.
- (12) Bonifazi, D.; Fasano, F.; Lorenzo-García, M. M.; Marinelli, D.; Oubaha, H.; Tasseroul, J. *Chem. Commun.* **2015**, *51*, 15222–15236.
- (13) Noda, H.; Furutachi, M.; Asada, Y.; Shibasaki, M.; Kumagai, N. *Nat. Chem.* **2017**, DOI: 10.1038/nchem.2708.
- (14) Edel, K.; Brough, S. A.; Lamm, A. N.; Liu, S.-Y.; Bettinger, H. F. *Angew. Chem., Int. Ed.* **2015**, *54*, 7819–7822.
- (15) Xu, S.; Mikulas, T. C.; Zakharov, L. N.; Dixon, D. A.; Liu, S.-Y. *Angew. Chem., Int. Ed.* **2013**, *52*, 7527–7531.
- (16) Braunschweig, H.; Celik, M. A.; Hupp, F.; Krummenacher, I.; Mailänder, L. *Angew. Chem., Int. Ed.* **2015**, *54*, 6347–6351.
- (17) Marwitz, A. J. V.; Lamm, A. N.; Zakharov, L. N.; Vasiliu, M.; Dixon, D. A.; Liu, S.-Y. *Chem. Sci.* **2012**, *3*, 825–829.
- (18) Lamm, A. N.; Garner, E. B.; Dixon, D. A.; Liu, S.-Y. *Angew. Chem., Int. Ed.* **2011**, *50*, 8157–8160.
- (19) Campbell, P. G.; Abbey, E. R.; Neiner, D.; Grant, D. J.; Dixon, D. A.; Liu, S.-Y. *J. Am. Chem. Soc.* **2010**, *132*, 18048–18050.
- (20) Liu, L.; Marwitz, A. J. V.; Matthews, B. W.; Liu, S.-Y. *Angew. Chem., Int. Ed.* **2009**, *48*, 6817–6819.
- (21) Hatakeyama, T.; Hashimoto, S.; Oba, T.; Nakamura, M. *J. Am. Chem. Soc.* **2012**, *134*, 19600–19603.
- (22) Wang, X.-Y.; Lin, H.-R.; Lei, T.; Yang, D.-C.; Zhuang, F.-D.; Wang, J.-Y.; Yuan, S.-C.; Pei, J. *Angew. Chem., Int. Ed.* **2013**, *52*, 3117–3120.
- (23) Braunschweig, H.; Damme, A.; Jimenez-Halla, J. O. C.; Pfaffinger, B.; Radacki, K.; Wolf, J. *Angew. Chem., Int. Ed.* **2012**, *51*, 10034–10037.
- (24) Agou, T.; Sekine, M.; Kobayashi, J.; Kawashima, T. *Chem. Commun.* **2009**, *16*, 1894–1896.
- (25) Kranz, M.; Hampel, F.; Clark, T. J. *Chem. Soc. Chem. Commun.* **1992**, *42*, 1247–1248.
- (26) Helten, H. *Chem. Eur. J.* **2016**, *22*, 12972–12982.
- (27) Jäkle, F. *Chem. Rev.* **2010**, *110*, 3985–4022.
- (28) Jäkle, F. Recent Advances in the Synthesis and Applications of Organoborane Polymers. In *Synthesis and Application of Organoboron Compounds*; Fernández, E.; Whiting, A., Eds.; Springer International Publishing: Basel, 2015; 49, pp 297–325.
- (29) Lorenz, T.; Crumbach, M.; Eckert, T.; Lik, A.; Helten, H. *Angew. Chem., Int. Ed.* **2017**, *56*, 2780–2784.
- (30) Ayhan, O.; Eckert, T.; Plamper, F. A.; Helten, H. *Angew. Chem., Int. Ed.* **2016**, *55*, 13321–13325.
- (31) Lorenz, T.; Lik, A.; Plamper, F. A.; Helten, H. *Angew. Chem., Int. Ed.* **2016**, *55*, 7236–7241.
- (32) Wan, W.-M.; Baggett, A. W.; Cheng, F.; Lin, H.; Liu, S.-Y.; Jäkle, F. *Chem. Commun.* **2016**, *52*, 13616–13619.
- (33) Baggett, A. W.; Guo, F.; Li, B.; Liu, S.-Y.; Jäkle, F. *Angew. Chem., Int. Ed.* **2015**, *54*, 1191–1195.
- (34) Côté, M.; Haynes, P. D.; Molteni, C. *Phys. Rev. B* **2001**, *63*, 125207.
- (35) Türker, L. *Polycycl. Aromat. Compd.* **2012**, *32*, 61–74.
- (36) Otero, N.; El-kelany, K. E.; Pouchan, C.; Rérat, M.; Karamanis, P. *Phys. Chem. Chem. Phys.* **2016**, *18*, 25315–25328.
- (37) Otero, N.; Karamanis, P.; El-Kelany, K. E.; Rérat, M.; Maschio, L.; Civalieri, B.; Kirtman, B. *J. Phys. Chem. C* **2017**, *121*, 709–722.
- (38) Culling, G. C.; Dewar, M. J. S.; Marr, P. A. *J. Am. Chem. Soc.* **1964**, *86*, 1125–1127.
- (39) Hatakeyama, T.; Hashimoto, S.; Seki, S.; Nakamura, M. *J. Am. Chem. Soc.* **2011**, *133*, 18614–18617.
- (40) Wakamiya, A.; Ide, T.; Yamaguchi, S. *J. Am. Chem. Soc.* **2005**, *127*, 14859–14866.
- (41) Hashimoto, S.; Ikuta, T.; Shiren, K.; Nakatsuka, S.; Ni, J.; Nakamura, M.; Hatakeyama, T. *Chem. Mater.* **2014**, *26*, 6265–6271.
- (42) Bosdet, M. J., Jaska, C. A., Piers, W. E., Sorensen, T. S., & Parvez, M.; Bosdet, M.; Jaska, C.; Piers, W.; Sorensen, T. *Org. Lett.* **2007**, *9*, 1395–1398.
- (43) Bosdet, M. J. D.; Piers, W. E.; Sorensen, T. S.; Parvez, M. *Angew. Chem., Int. Ed.* **2007**, *46*, 4940–4943.
- (44) Kalashnyk, N.; Ganesh Nagaswaran, P.; Kervyn, S.; Riello, M.; Moreton, B.; Jones, T. S.; De Vita, A.; Bonifazi, D.; Costantini, G. *Chem. Eur. J.* **2014**, *20*, 11856–11862.
- (45) Sham, I. H. T.; Kwok, C.-C.; Che, C.-M.; Zhu, N. *Chem. Commun.* **2005**, *2*, 3547–3549.
- (46) Urgel, J. I.; Schwarz, M.; Garnica, M.; Stassen, D.; Bonifazi, D.; Ecija, D.; Barth, J. V.; Auwärter, W. *J. Am. Chem. Soc.* **2015**, *137*, 2420–2423.
- (47) Kervyn, S.; Fenwick, O.; Di Stasio, F.; Shin, Y. S.; Wouters, J.; Accorsi, G.; Osella, S.; Beljonne, D.; Cacialli, F.; Bonifazi, D. *Chem. Eur. J.* **2013**, *19*, 7771–7779.
- (48) Ci, L.; Song, L.; Jin, C.; Jariwala, D.; Wu, D.; Li, Y.; Srivastava, A.; Wang, Z. F.; Storr, K.; Balicas, L.; Liu, F.; Ajayan, P. M. *Nat. Mater.*

- 2010, 9, 430–435.
- (49) Sánchez-Sánchez, C.; Brüller, S.; Sachdev, H.; Brüller, S.; Sachdev, H.; Müllen, K.; Krieg, M.; Bettinger, H. F.; Nicolai, A.; Meunier, V.; Talirz, L.; Fasel, R.; Ruffieux, P. *ACS Nano* **2015**, 9, 9228–9235.
- (50) Krieg, M.; Reichert, F.; Haiss, P.; Ströbele, M.; Eichele, K.; Treanor, M.-J.; Schaub, R.; Bettinger, H. F. *Angew. Chem., Int. Ed.* **2015**, 54, 8284–8286.
- (51) Ciccullo, F.; Calzolari, A.; Piš, I.; Savu, S.-A.; Krieg, M.; Bettinger, H. F.; Magnano, E.; Chassé, T.; Casu, M. B. *J. Phys. Chem. C* **2016**, 120, 17645–17651.
- (52) Berresheim, A. J.; Müller, M.; Müllen, K. *Chem. Rev.* **1999**, 99, 1747–1785.
- (53) Grimsdale, A. A. C.; Müllen, K. *Angew. Chem., Int. Ed.* **2005**, 44, 5592–5629.
- (54) Türp, D.; Nguyen, T.-T.-T.; Baumgarten, M.; Müllen, K. *New J. Chem.* **2012**, 36, 282–298.
- (55) Geng, Y.; Fechtenkötter, A.; Müllen, K. *J. Mater. Chem.* **2001**, 11, 1634–1641.
- (56) Qin, T.; Zhou, G.; Scheiber, H.; Bauer, R. E.; Baumgarten, M.; Anson, C. E.; List, E. J. W.; Müllen, K. *Angew. Chem., Int. Ed.* **2008**, 47, 8292–8296.
- (57) Müllen, K. *ACS Nano* **2014**, 8, 6531–6541.
- (58) Chen, L.; Hernandez, Y.; Feng, X.; Müllen, K. *Angew. Chem., Int. Ed.* **2012**, 51, 7640–7654.
- (59) Dössel, L.; Gherghel, L.; Feng, X.; Müllen, K. *Angew. Chem., Int. Ed.* **2011**, 50, 2540–2543.
- (60) Nagasawa, K. *Inorg. Chem.* **1966**, 5, 442–445.
- (61) Morgenroth, F.; Reuther, E.; Müllen, K. *Angew. Chem., Int. Ed.* **1997**, 36, 631–634.
- (62) Kervyn, S.; Kalashnyk, N.; Riello, M.; Moreton, B.; Tasseroul, J.; Wouters, J.; Jones, T. S.; De Vita, A.; Costantini, G.; Bonifazi, D. *Angew. Chem., Int. Ed.* **2013**, 52, 7410–7414.
- (63) Groszós, S. J.; Stafiej, S. F. *J. Am. Chem. Soc.* **1958**, 80, 1357–1360.
- (64) Hyatt, J. A. *Org. Prep. Proced. Int.* **1991**, 23, 460–463.
- (65) Pauling, L. *Proc. Natl. Acad. Sci.* **1966**, 56, 1646–1652.
- (66) Pauling, L. *The Nature of the Chemical Bond*; Cornell University Press: New York, 1960.
- (67) Proñ, A.; Baumgarten, M.; Müllen, K. *Org. Lett.* **2010**, 12, 4236–4239.
- (68) Kurata, R.; Kaneda, K.; Ito, A. *Org. Lett.* **2017**, 19, 392–395.
- (69) Steeger, M.; Holzapfel, M.; Schmiedel, A.; Lambert, C. *Phys. Chem. Chem. Phys.* **2016**, 18, 13403–13412.
- (70) Ji, L.; Griesbeck, S.; Marder, T. B. *Chem. Sci.* **2017**, 8, 846–863.
- (71) Hammer, B. A. G.; Müllen, K. *Chem. Rev.* **2016**, 116, 2103–2140.
- (72) Hecht, S.; Fréchet, J. M. J. *Angew. Chem., Int. Ed.* **2001**, 40, 74–91.
- (73) Mei, J.; Leung, N. L. C.; Kwok, R. T. K.; Lam, J. W. Y.; Tang, B. Z. *Chem. Rev.* **2015**, 115, 11718–11940.
- (74) Baroncini, M.; Bergamini, G.; Ceroni, P. *Chem. Commun.* **2017**, 53, 2081–2093.
- (75) Liu, D.; De Feyter, S.; Cotlet, M.; Stefan, A.; Wiesler, U.-M.; Herrmann, A.; Grebel-Koehler, D.; Qu, J.; Müllen, K.; De Schryver, F. C. *Macromolecules* **2003**, 36, 5918–5925.
- (76) Naomi Sakai; Jiri Mareda; Eric Vauthey; Stefan Matile; Sakai, N.; Mareda, J.; Vauthey, E.; Matile, S. *Chem. Commun.* **2010**, 46, 4225–4237.
- (77) Suraru, S. S. L.; Würthner, F. *Angew. Chem., Int. Ed.* **2014**, 53, 7428–7448.
- (78) Berezin, A. A.; Scitutto, A.; Demitri, N.; Bonifazi, D. *Org. Lett.* **2015**, 17, 1870–1873.
- (79) Melinger, J. J. S.; Pan, Y.; Kleiman, V. V. D.; Peng, Z.; Davis, B. L.; McMorro, D.; Lu, M. J. *Am. Chem. Soc.* **2002**, 124, 12002–12012.
- (80) Weil, T.; Vosch, T.; Hofkens, J.; Peneva, K.; Müllen, K. *Angew. Chem., Int. Ed.* **2010**, 49, 9068–9093.
- (81) Qu, J.; Pschirer, N. G.; Liu, D.; Stefan, A.; De Schryver, F. C.; Müllen, K. *Chem. Eur. J.* **2004**, 10, 528–537.
- (82) Qu, J.; Zhang, J.; Grimsdale, A. C.; Müllen, K.; Jaiser, F.; Yang, X.; Neher, D. *Macromolecules* **2004**, 37, 8297–8306.

